Electronic Supplementary Material (ESI) for RSC Advances.

New Iboga-Type Alkaloids from *Ervatamia hainanensis*

Zhi-Wen Liu,‡[ab] Xiao-Jun Huang,‡[ab] Han-Lin Xiao,[b] Guo Liu,[ab] Jian Zhang,[ab] Lei Shi,[b] Ren-Wang Jiang,[ab] Xiao-Qi Zhang[ab]* and Wen-Cai Ye[ab]*

[a] Institute of Traditional Chinese Medicine and Natural Products, College of Pharmacy, Jinan University, Guangzhou 510632, P. R. China.

[b] Guangdong Province Key Laboratory of Pharmacodynamic Constituents of TCM and New Drugs Research, Jinan University, Guangzhou 510632, P. R. China.

Corresponding author: Tel. (fax): +86 20 8522 3994

Email: tzhxq01@jnu.com.cn (X. Q. Zhang), chyewc@gmail.com (W. C. Ye)

List of Supporting Information

1. Single crystal X-ray crystallographic analysis of 1,4,6 and 9

The structures were solved by direct methods and refined by full-matrix least-squares on F^2 using SHELXL-97 package software. Crystallographic data have been deposited with the Cambridge Crystallographic Data Centre as deposition number CCDC 1444994 for **1**, CCDC 1444995 for **4**, CCDC 1444996 for **6** and CCDC 1444997 for **9**.

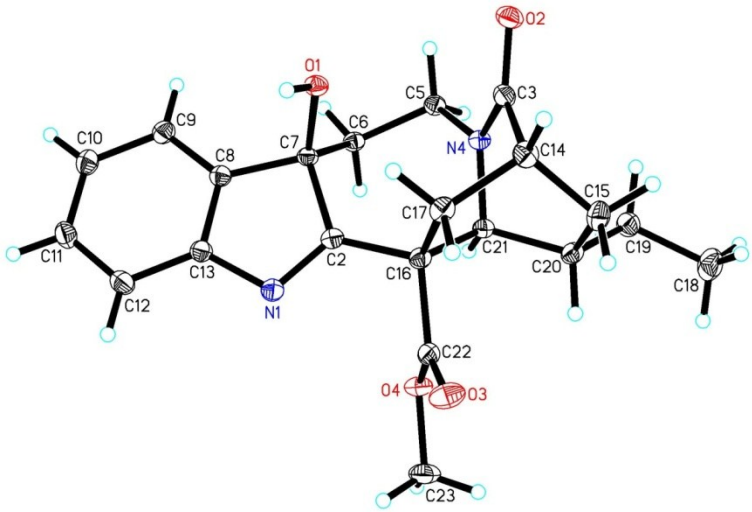

Fig. S1 X-ray crystal structure of **1**

X-ray crystallographic data of 1: $C_{21}H_{24}N_2O_4 \cdot C_2H_3N$ (fw = 409.48); Monoclinic, space group $P2_1$; a = 10.07340(18) Å, b = 9.87893(13) Å, c = 11.00555(18) Å, α =90°, β = 107.6571(19)°, γ = 90°; V = 1043.61(3) Å^3, T = 173(2) K, Z = 2, D_c = 1.303 g/cm^3, F(000) = 436. A total of 16047 reflections were collected in the range $5.22 \leq \theta \leq 62.73$, of which 3274 unique reflections with $I > 2\sigma(I)$ were collected for the analysis. Final R = 0.0243 and R_w =0.0634, and the goodness of fit on F^2 was equal to 1.048; Flack parameter = 0.04(13). Crystallographic data for the structure reported in this paper had been deposited at the Cambridge Crystallographic Data Centre under the reference number CCDC

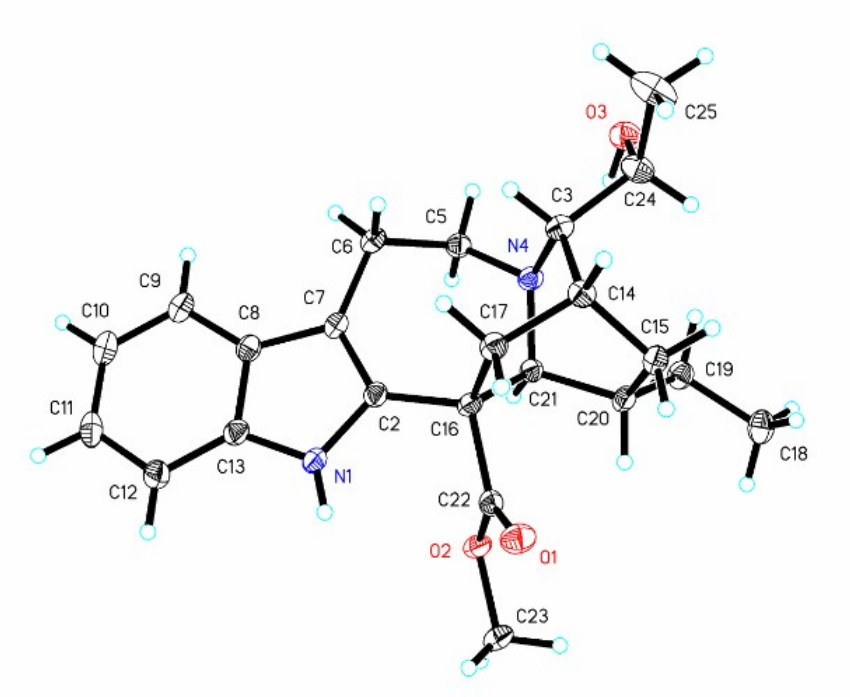

Fig. S2 X-ray crystal structure of **4**

X-ray crystallographic data of 4: $C_{23}H_{30}N_2O_3$ (fw = 382.49); Monoclinic, space group $P2_1$; a = 9.7015(8) Å, b = 10.7426(8) Å, c = 10.0282(10) Å, α =90°, β = 107.663(10)°, γ = 90°; V = 995.86(16) Å^3, T = 173(2) K, Z = 2, D_c = 1.276 g/cm^3, F(000) = 418. A total of 4010 reflections were collected in the range 4.63 ≤ θ ≤ 62.72, of which 2101 unique reflections with $I > 2\sigma(I)$ were collected for the analysis. Final R = 0.0468 and R_w = 0.1104, and the goodness of fit on F^2 was equal to 1.071; Flack parameter = 0.0(4).

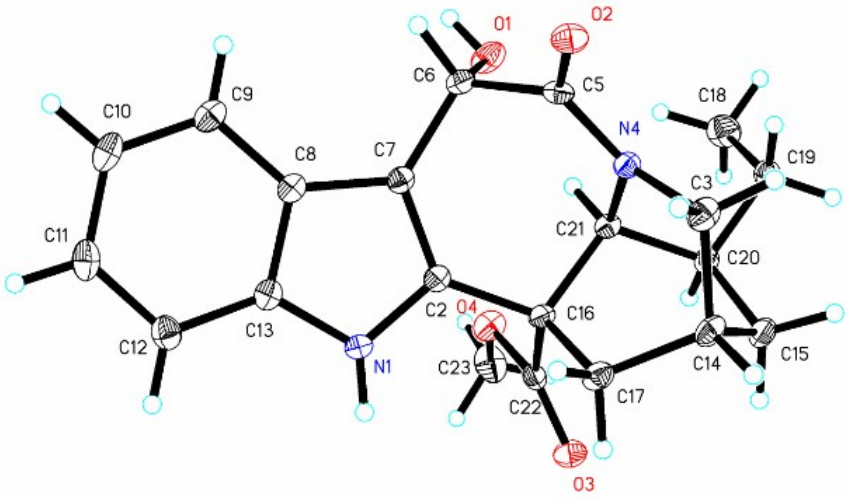

Fig. S3 X-ray crystal structure of **6**

X-ray crystallographic data of 6: $C_{21}H_{24}N_2O_4$ (fw = 368.42); Orthorhombic, space group $P2_12_12_1$; a = 7.44984(14) Å, b = 11.4893(2) Å, c = 21.3736(4) Å, $\alpha = \beta = \gamma = 90°$; V = 1829.44(6) Å^3, T = 173(2) K, Z= 4, D_c = 1.338 g/cm^3, F(000) = 784. A total of 14469 reflections were collected in the range $4.37 \leq \theta \leq 62.70$, of which 2879 unique reflections with $I > 2\sigma(I)$ were collected for the analysis. Final R = 0.0262 and R_w = 0.0676, and the goodness of fit on F^2 was equal to 1.084; Flack parameter = 0.01(6).

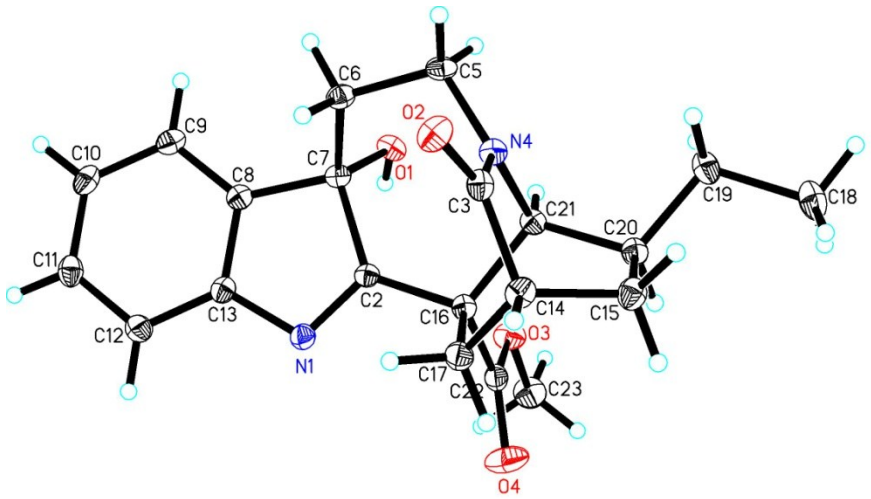

Fig. S4 X-ray crystal structures of **9**

X-ray crystallographic data of 9: $C_{21}H_{24}N_2O_4$ (fw = 368.42); Orthorhombic, space group $P2_12_12_1$; a = 8.78022(19) Å, b = 13.8217(4) Å, c = 15.0748(4) Å, $a = \beta = \gamma = 90°$; V = 1829.43(8) Å^3, T = 173(10) K, Z = 4, D_c = 1.338 g/cm^3, $F(000)$ = 784. A total of 14636 reflections were collected in the range $4.33 \leq \theta \leq 62.94$, of which 2827 unique reflections with $I > 2\sigma(I)$ were collected for the analysis. Final R = 0.0289 and R_w = 0.0703, and the goodness of fit on F^2 was equal to 1.066; Flack parameter = 0.13(9)

2. Effects of the compounds on cell viability

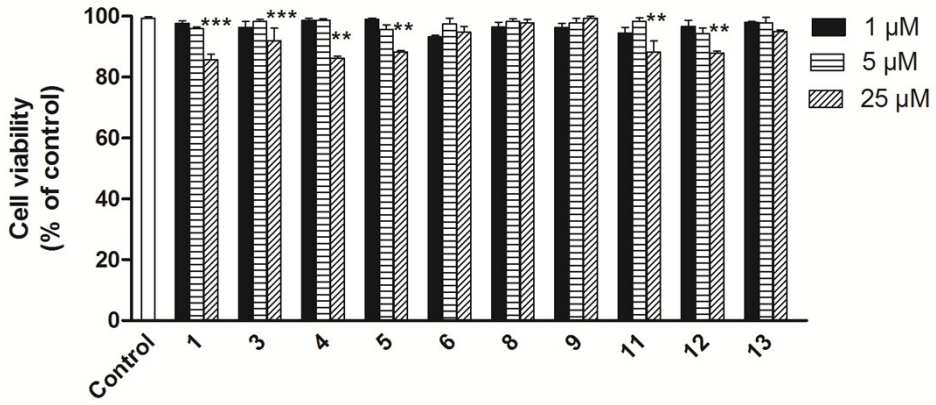

Fig. S5 Effects of the isolated alkaloids on cell viability. Neuro-2a cells were cultured in MEM (Invitrogen) supplied with 10% FBS plus antibiotics and seeded in 96-well plates (8 × 10^3/well). Neuron-2a cells were treated with different alkaloids at 1, 5 and 25 μM, and cell viability was measured at 24 h later. Data are shown as mean ± SEM of three experiments. $^*P < 0.05$ vs. DMSO. $^{**}P < 0.01$, $^{***}P < 0.001$, one-way ANOVA followed by Bonferroni's Multiple Comparison Test.

3. Effect of the compounds on corticosterone-induced neurotoxicity in PC12 cells

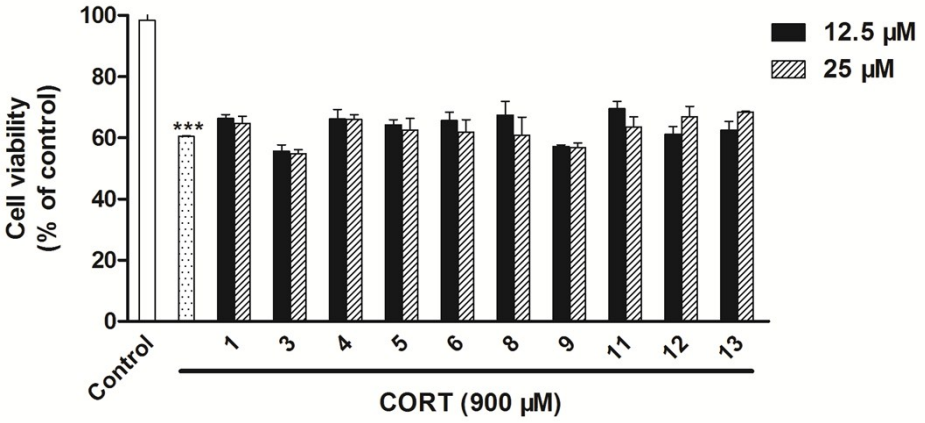

Fig. S6 The isolated alkaloids have no effects on corticosterone (CORT)-induced toxicity in PC12 cells. PC12 cells (ATCC, Manassas, VA, USA) were grown in DMEM supplemented with 6% FBS, and 6% HS plus antibiotics. Cells were treated with 900 μM CORT (purchased from Aladdin Reagents Company, Shanghai, China). With or without indicated alkaloid at different concentrations, and cell viability was measured at 24 h later. The results are expressed as mean ± SEM (n = 3) of three independent experiments. $^{***}P < 0.001$ as compared with control. One-way ANOVA followed by Bonferroni's Multiple Comparison Test.

4. UV, IR, HRESIMS, ECD and NMR spectra of 1-7

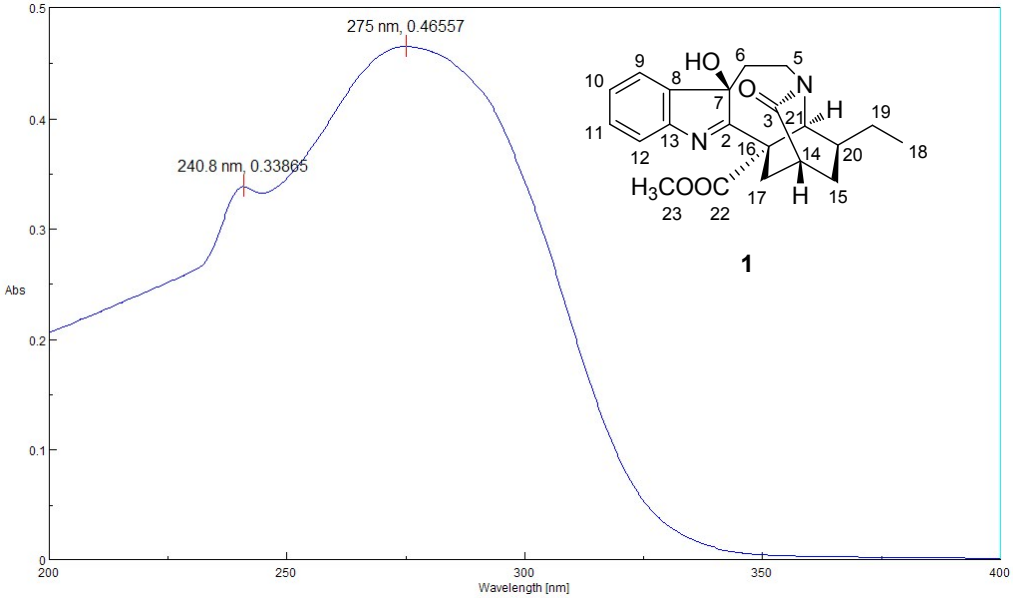

Fig. S7 UV spectrum of **1** ($CHCl_3$)

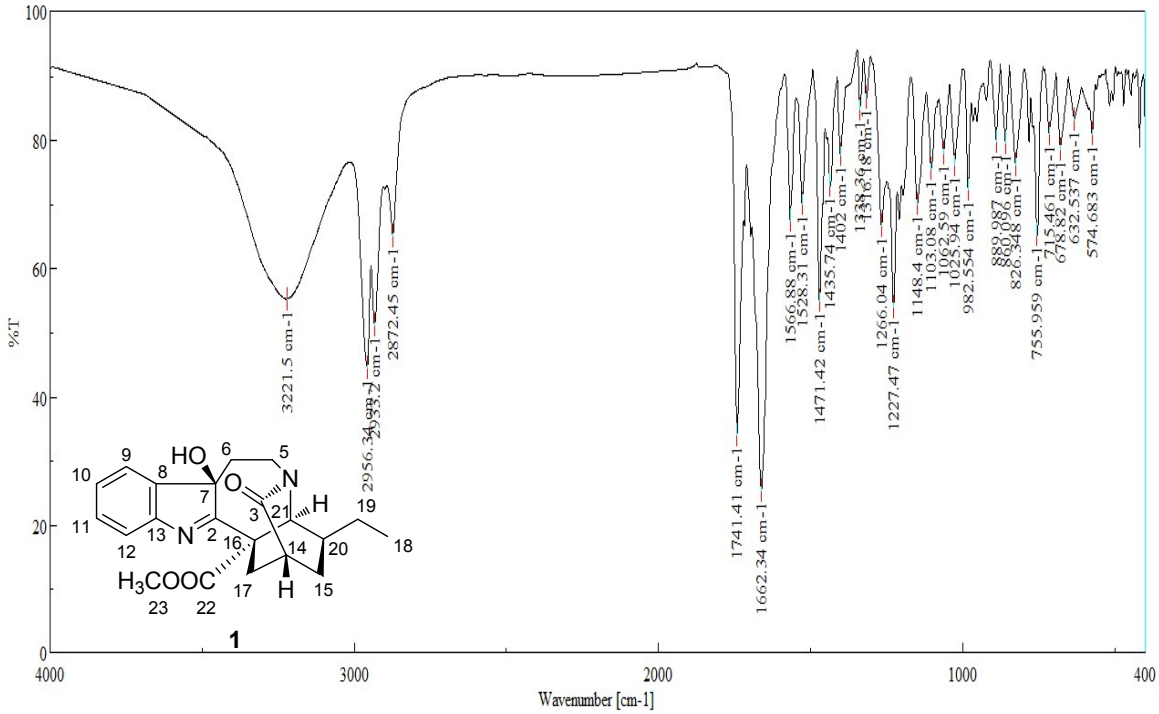

Fig. S8 IR spectrum of **1** (KBr)

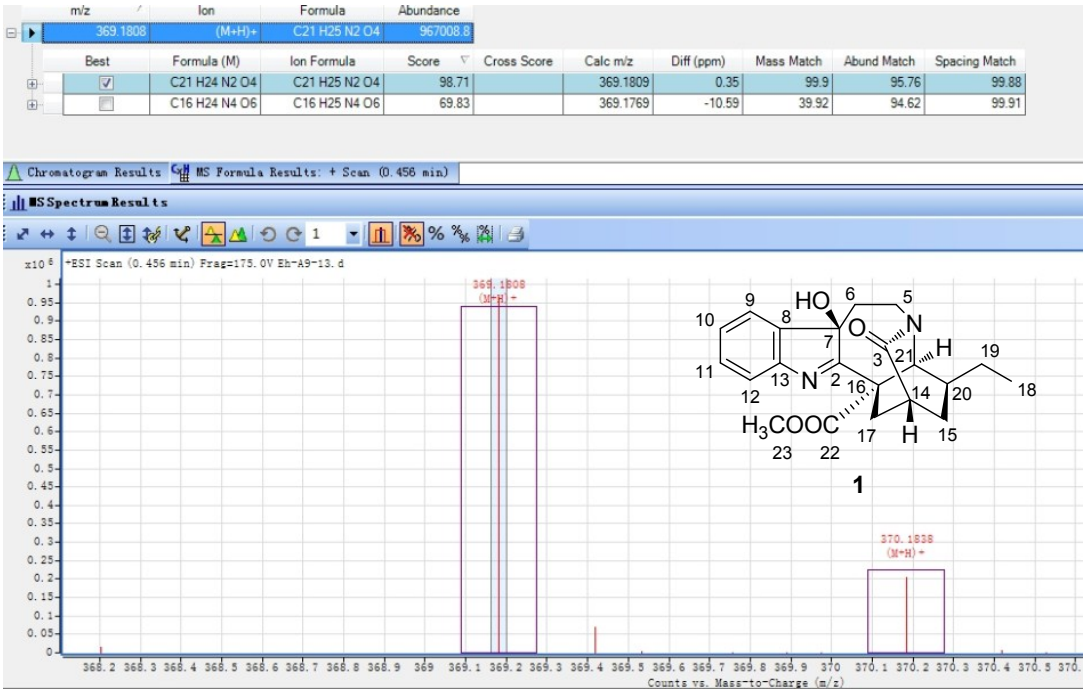

Fig. S9 HR-ESI-MS spectrum of **1**

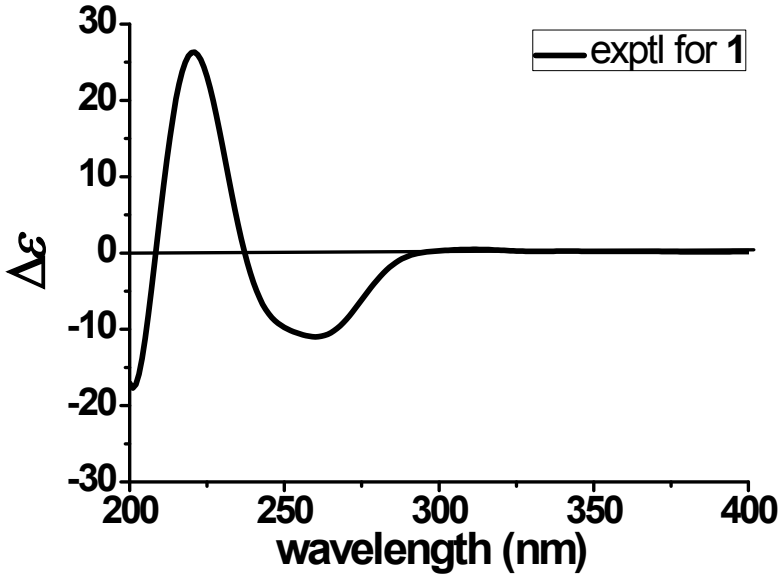

Fig. S10 ECD spectrum of **1** (CH_3CN)

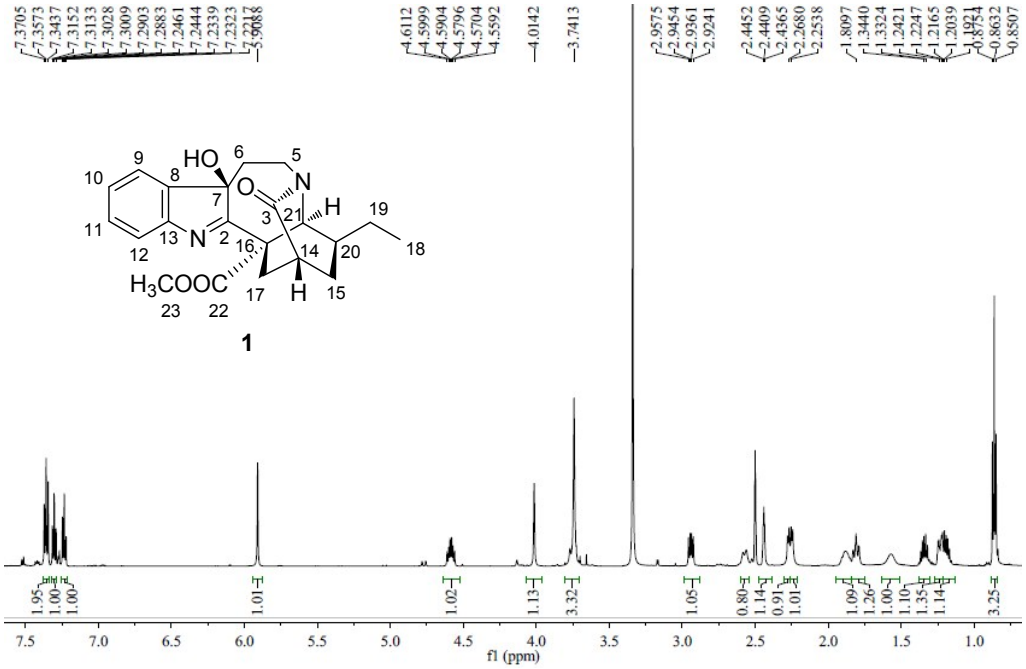

Fig. S11 ^{1}H-NMR spectrum of **1** (DMSO-d_6)

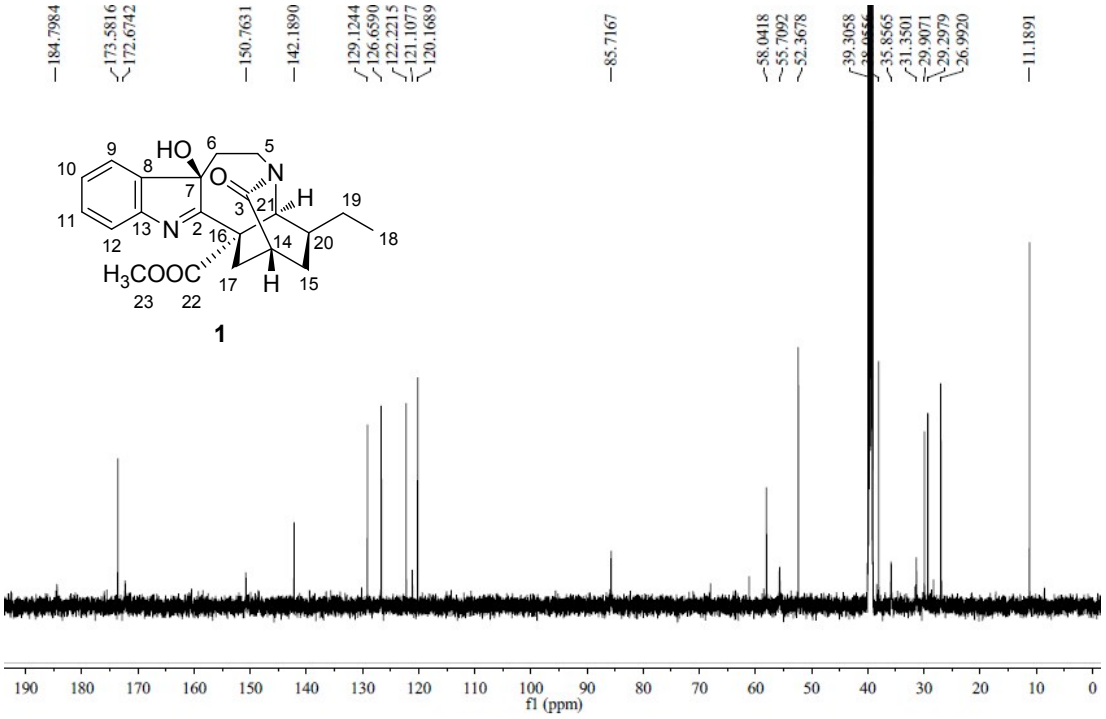

Fig. S12 ^{13}C-NMR spectrum of **1** (DMSO-d_6)

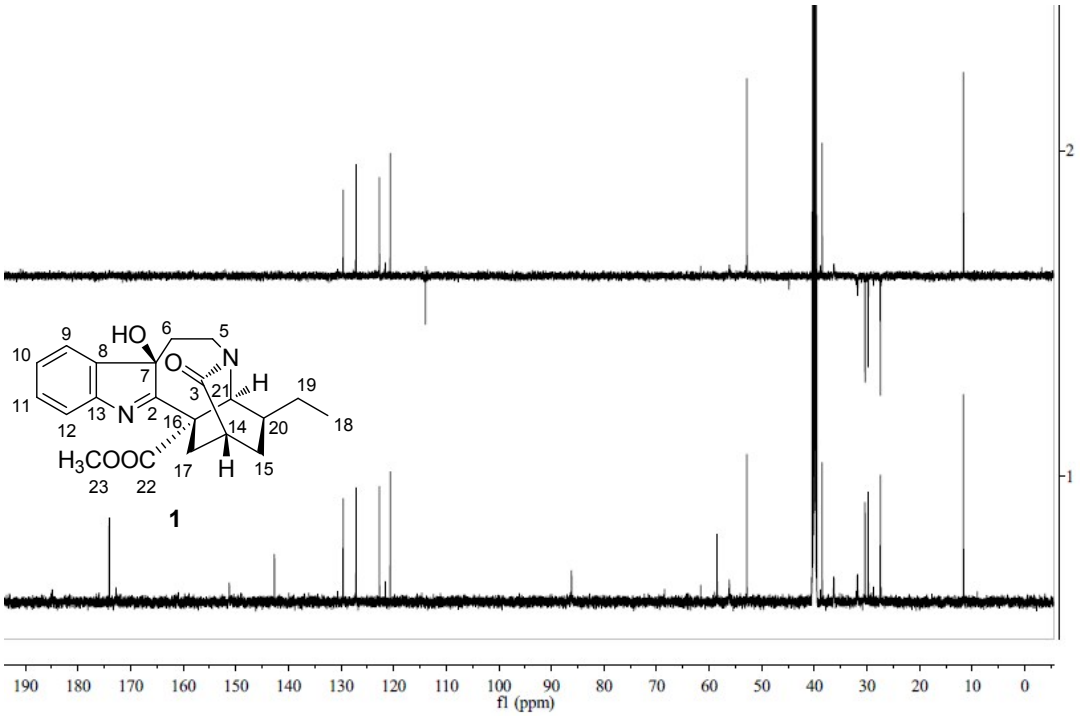

Fig. S13 DEPT-135 spectrum of **1** (DMSO-d_6)

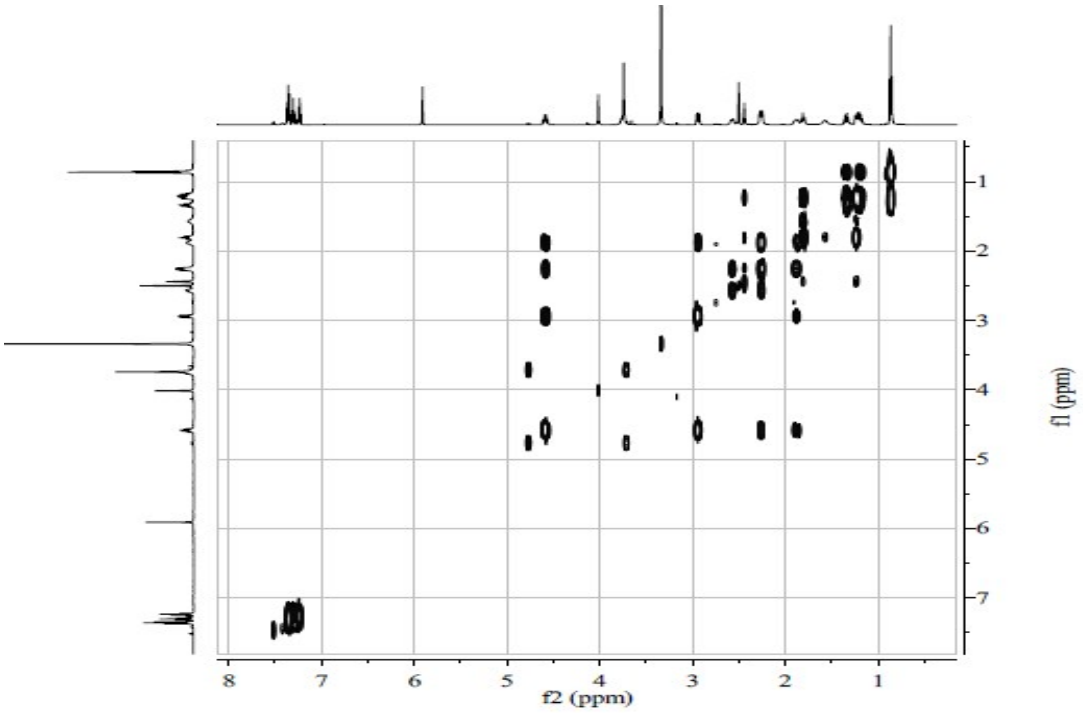

Fig. S14 ^{1}H-^{1}H COSY spectrum of **1** (DMSO-d_6)

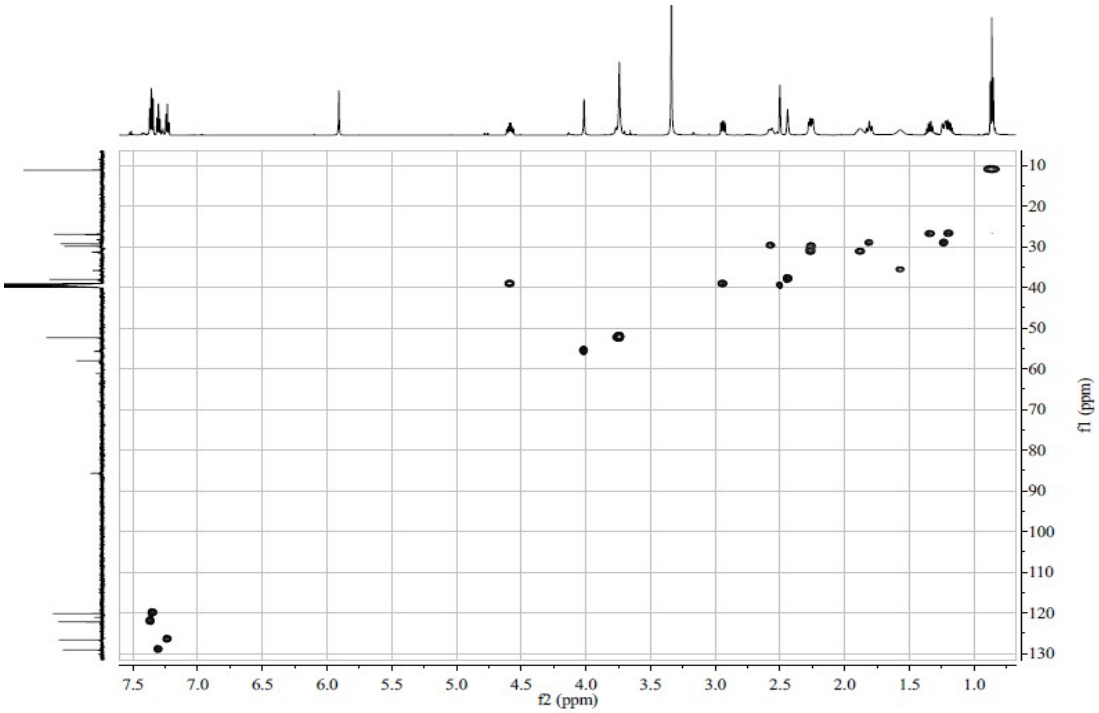

Fig. S15 HSQC spectrum of **1** (DMSO-d_6)

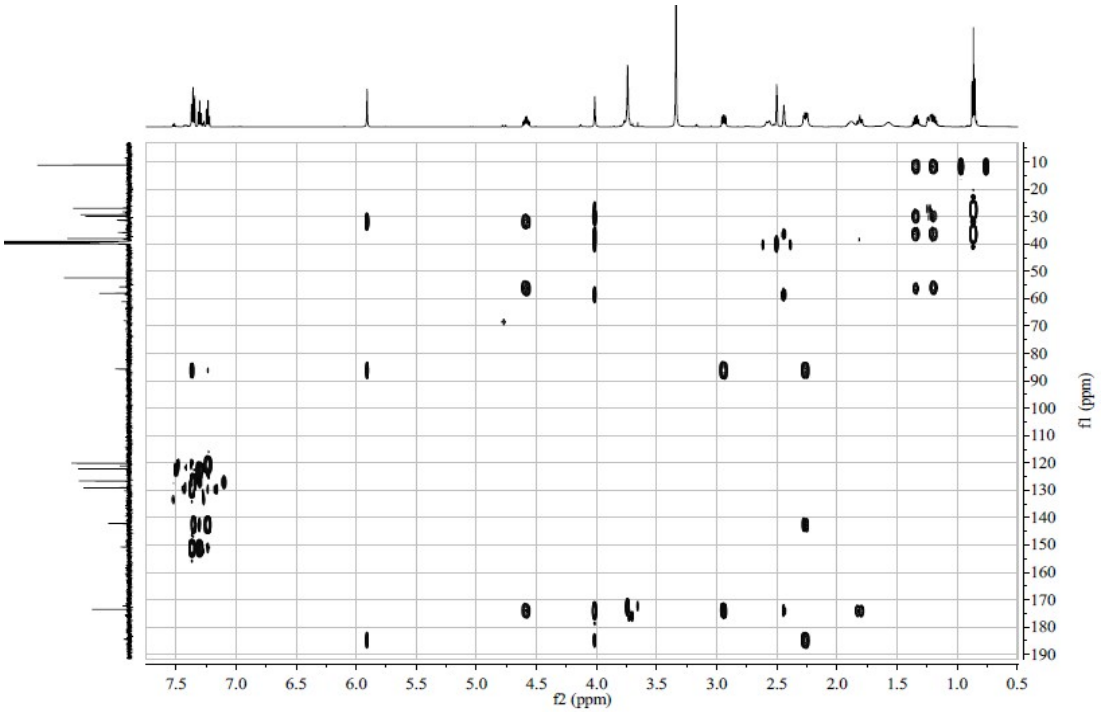

Fig. S16 HMBC spectrum of **1** (DMSO-d_6)

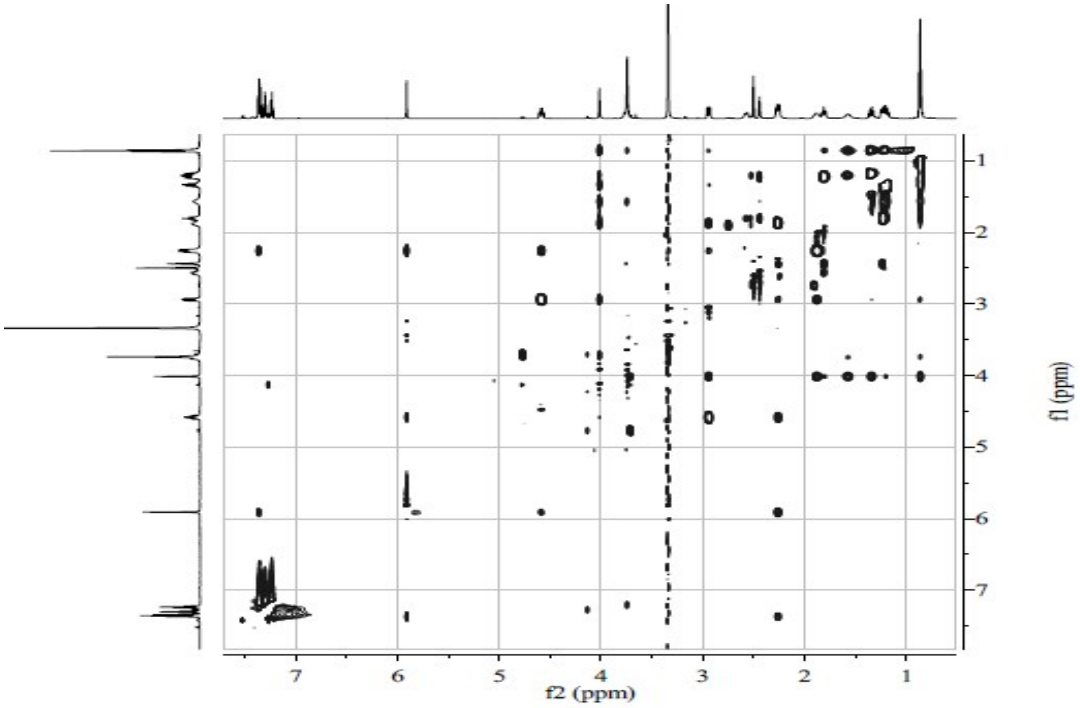

Fig. S17 NOESY spectrum of **1** (DMSO-d_6)

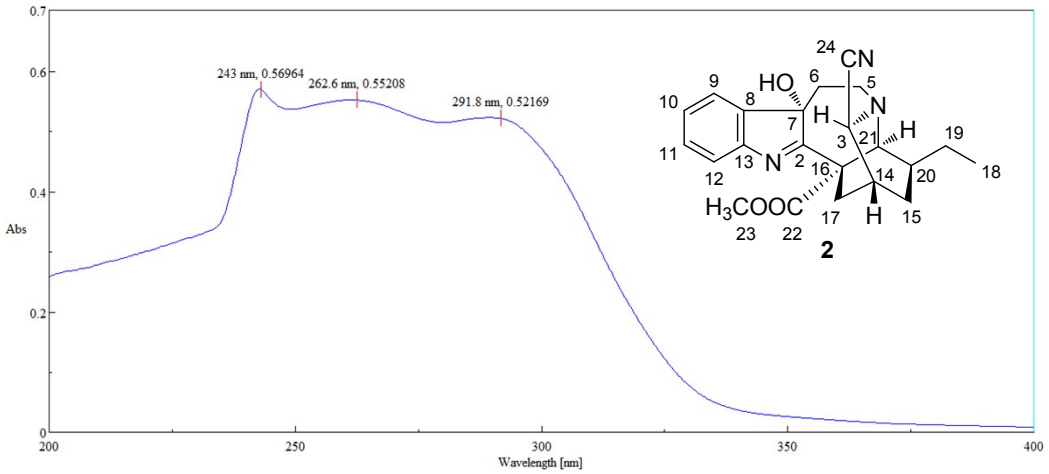

Fig. S18 UV spectrum of **2** ($CHCl_3$)

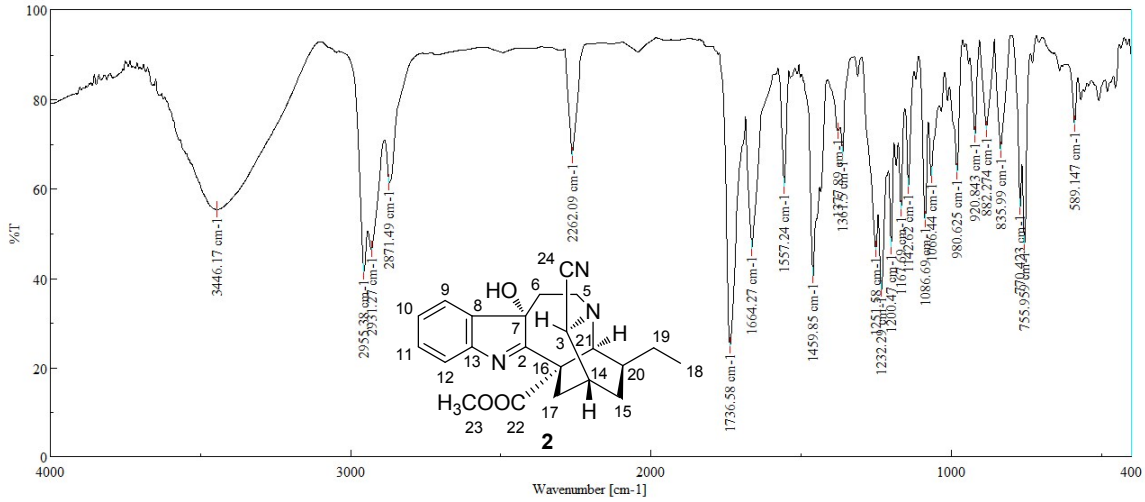

Fig. S19 IR spectrum of **2** (KBr)

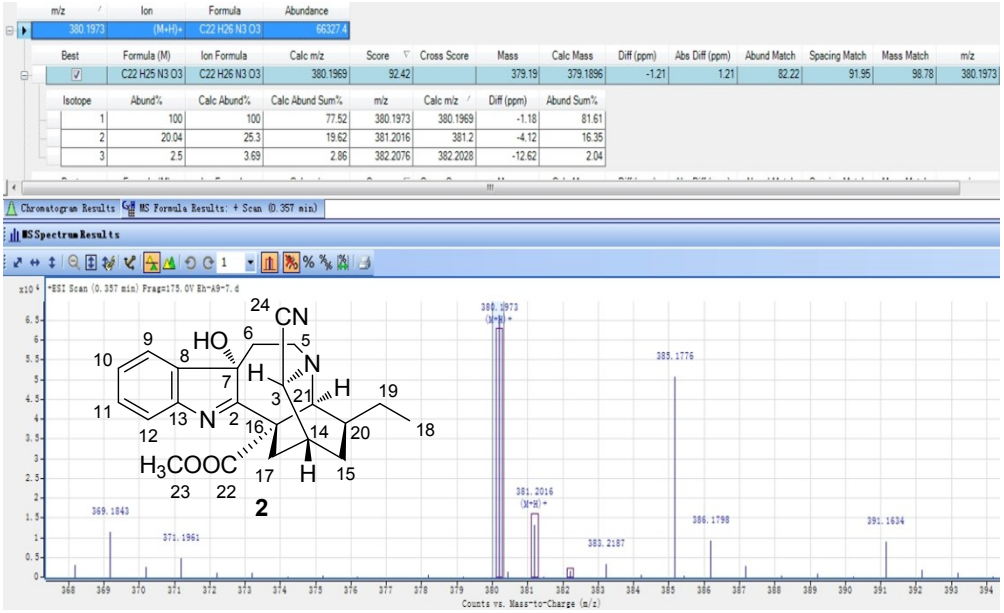

Fig. S20 HR-ESI-MS spectrum of **2**

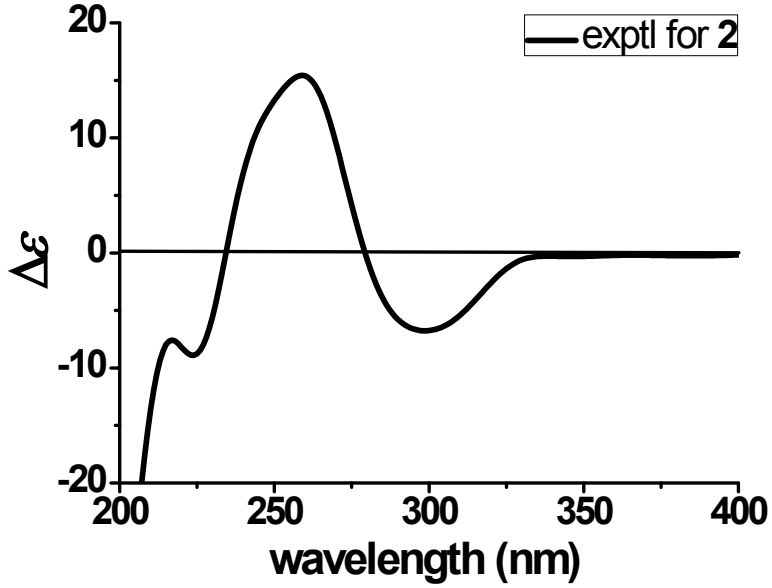

Fig. S21 ECD spectrum of **2** (CH_3CN)

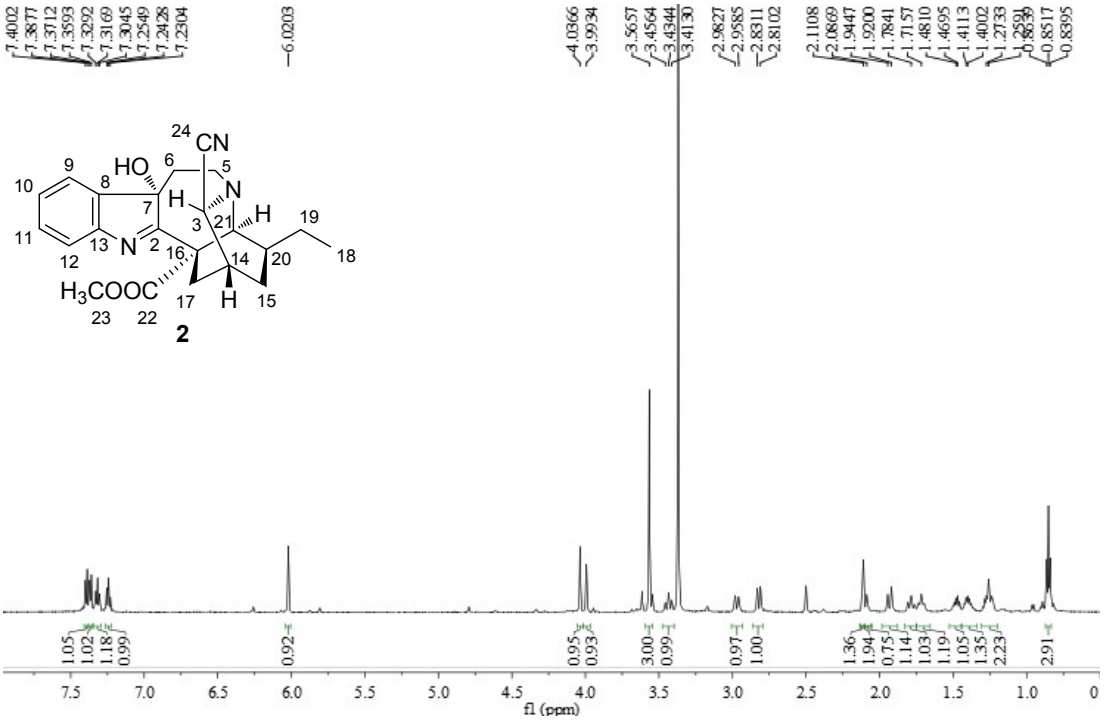

Fig. S22 ^{1}H-NMR spectrum of **2** (DMSO-d_6)

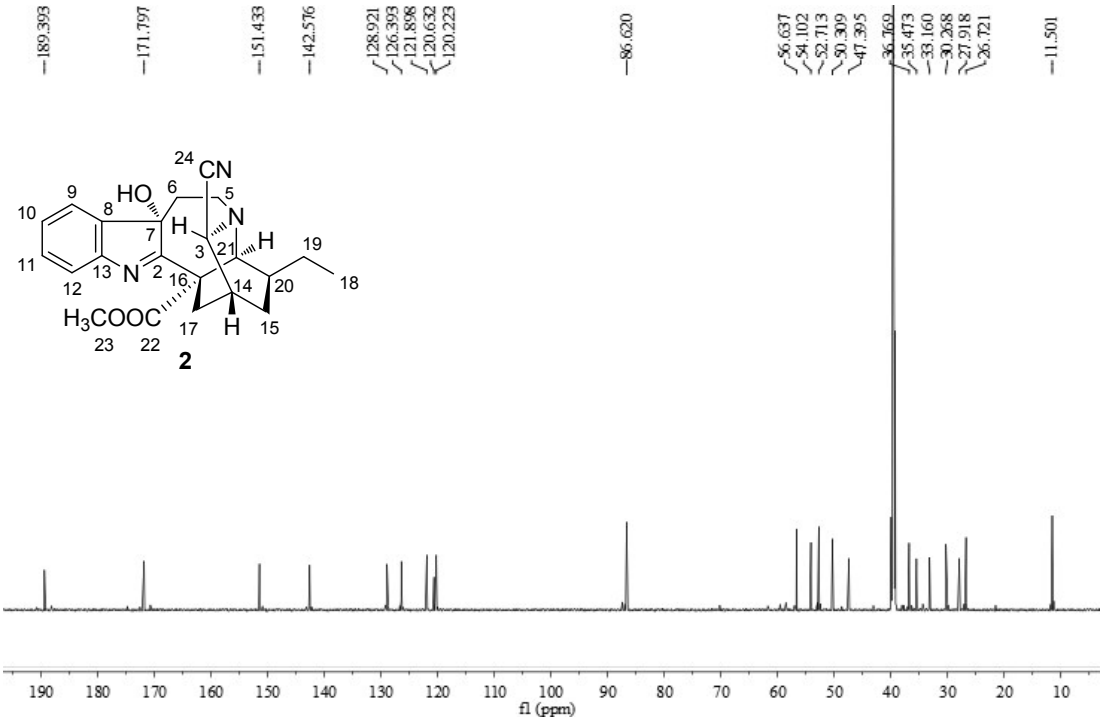

Fig. S23 ^{13}C-NMR spectrum of **2** (DMSO-d_6)

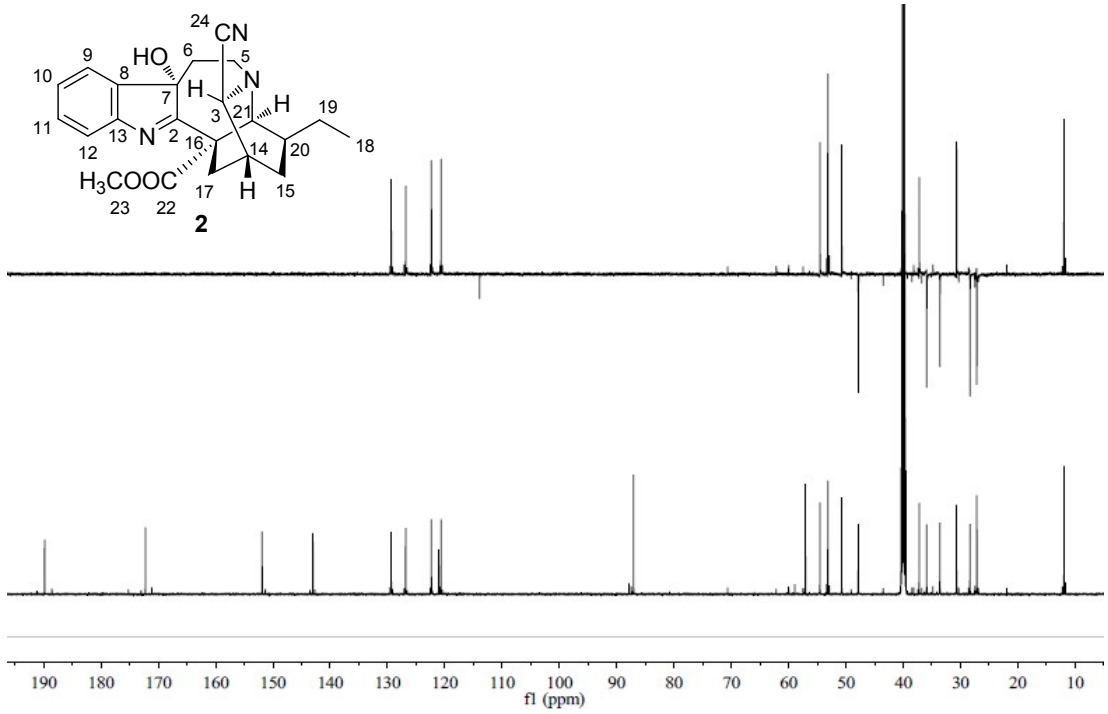

Fig. S24 DEPT-135 spectrum of **2** (DMSO-d_6)

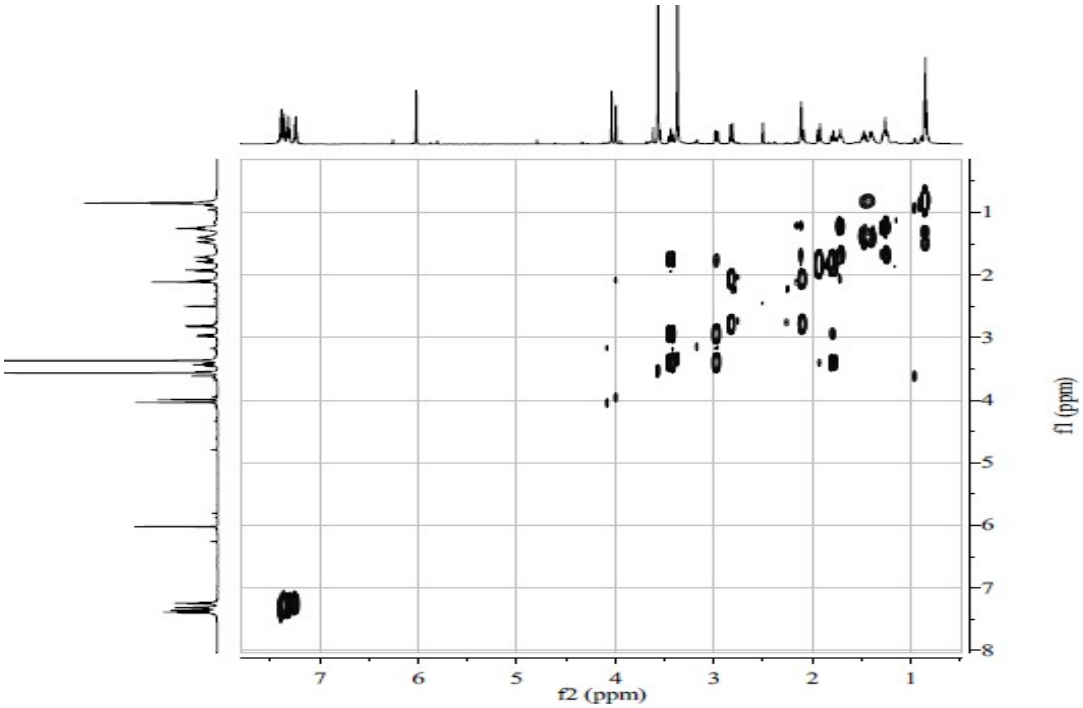

Fig. S25 ^{1}H-^{1}H COSY spectrum of **2** (DMSO-d_6)

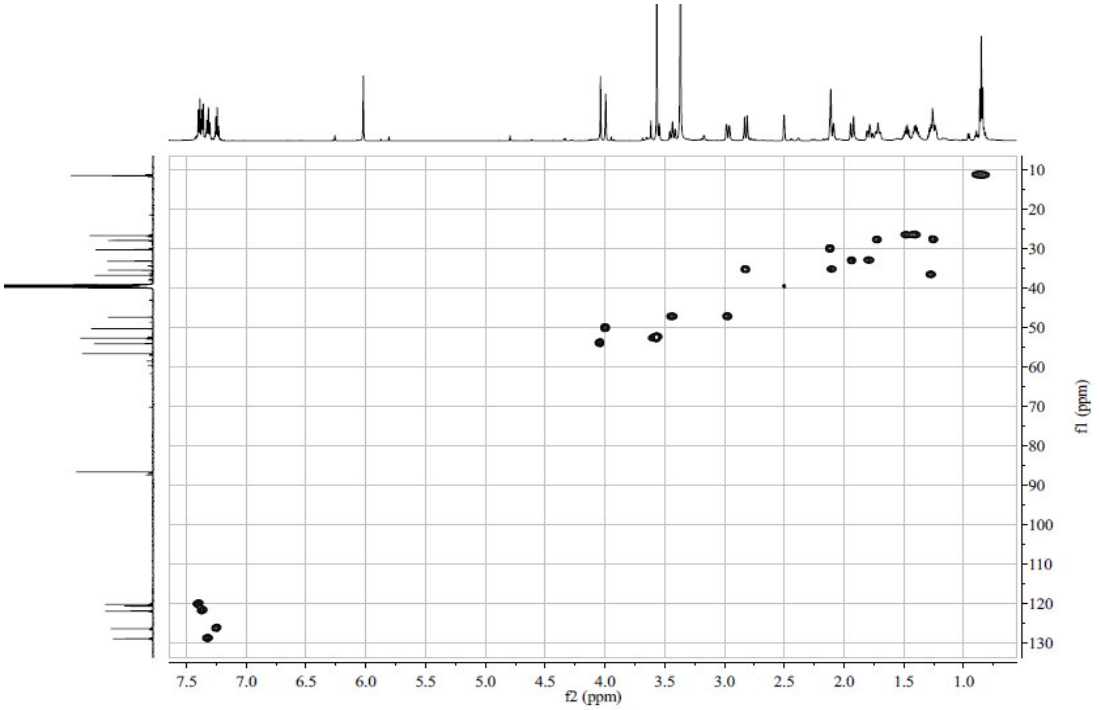

Fig. S26 HSQC spectrum of **2** (DMSO-d_6)

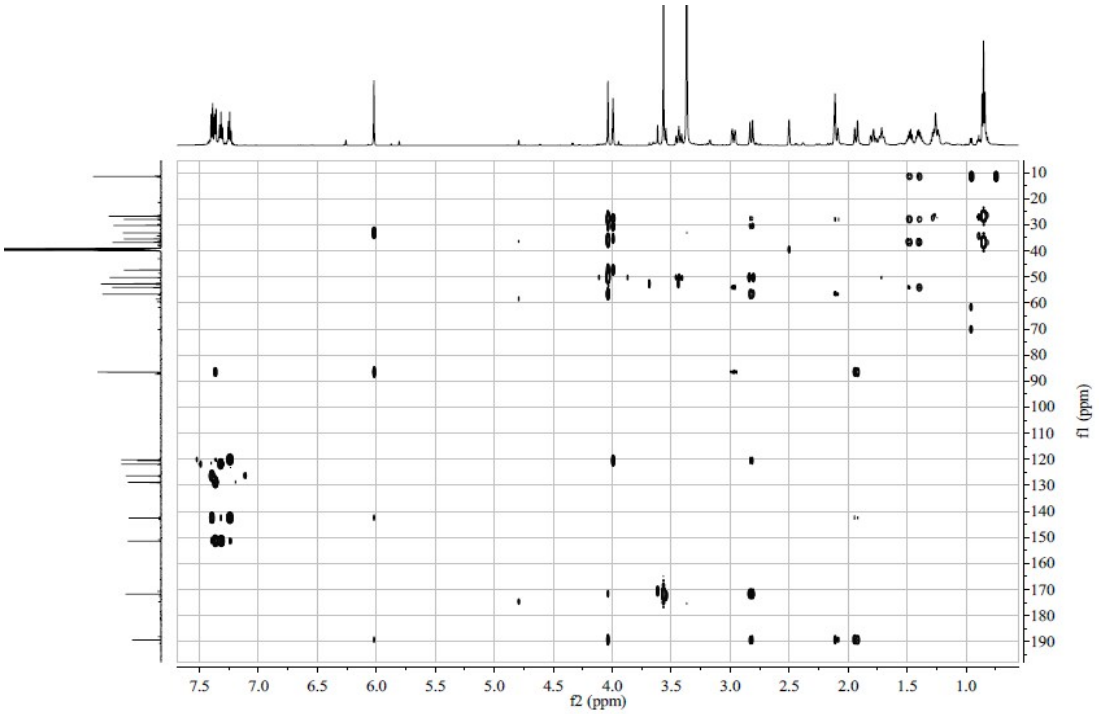

Fig. S27 HMBC spectrum of **2** (DMSO-d_6)

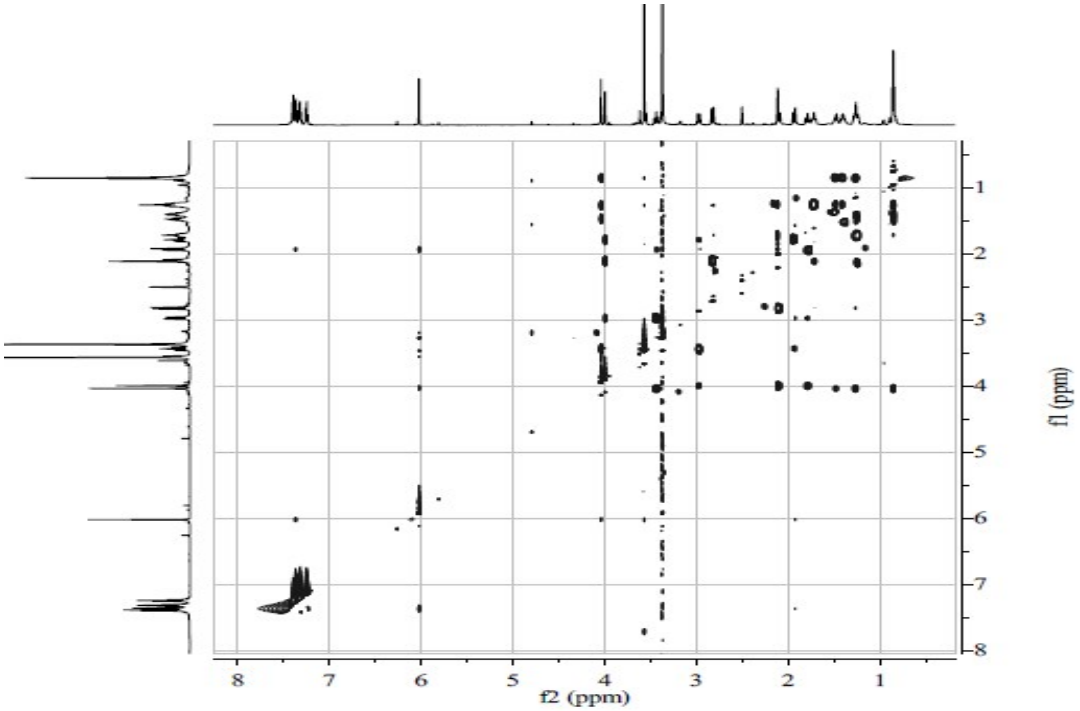

Fig. S28 NOESY spectrum of **2** (DMSO-d_6)

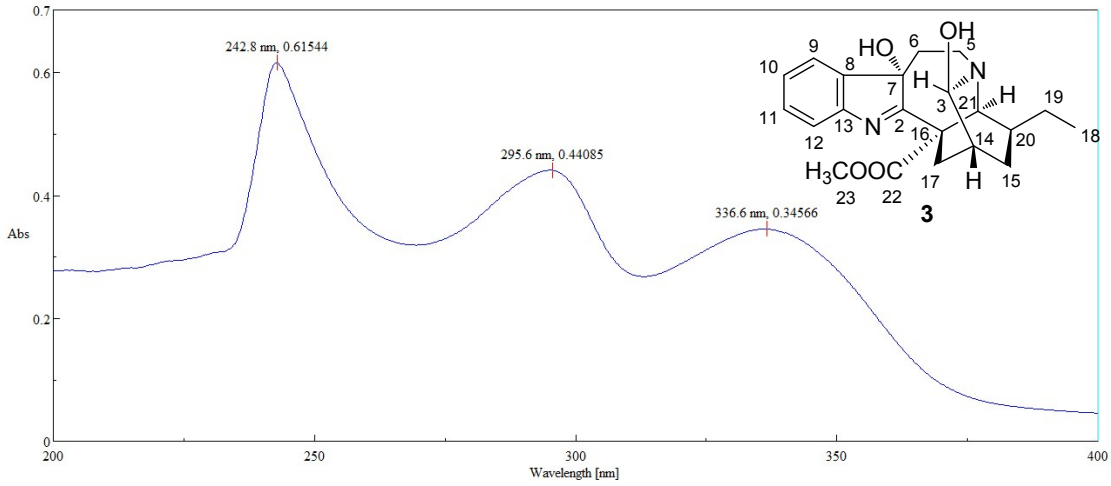

Fig. S29 UV spectrum of **3** ($CHCl_3$)

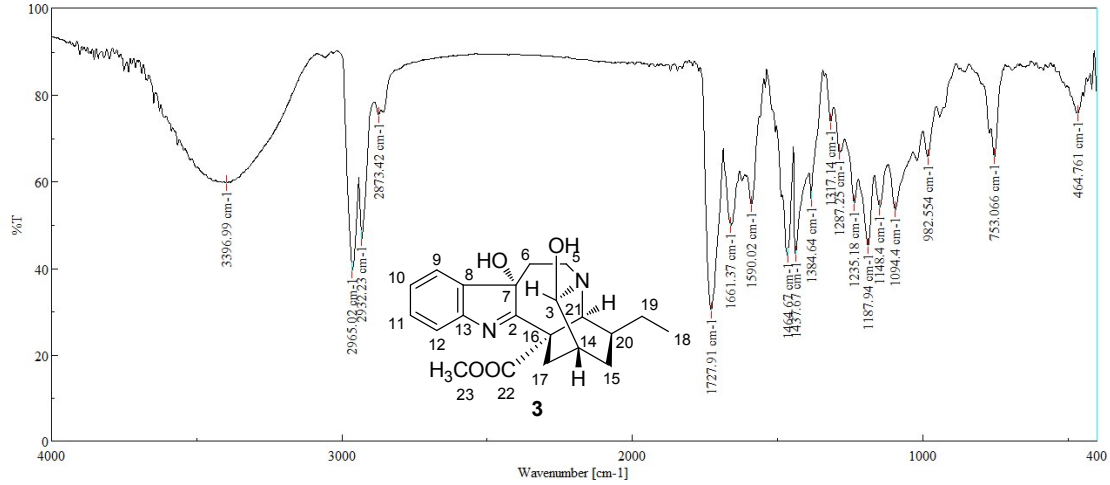

Fig. S30 IR spectrum of **3** (KBr)

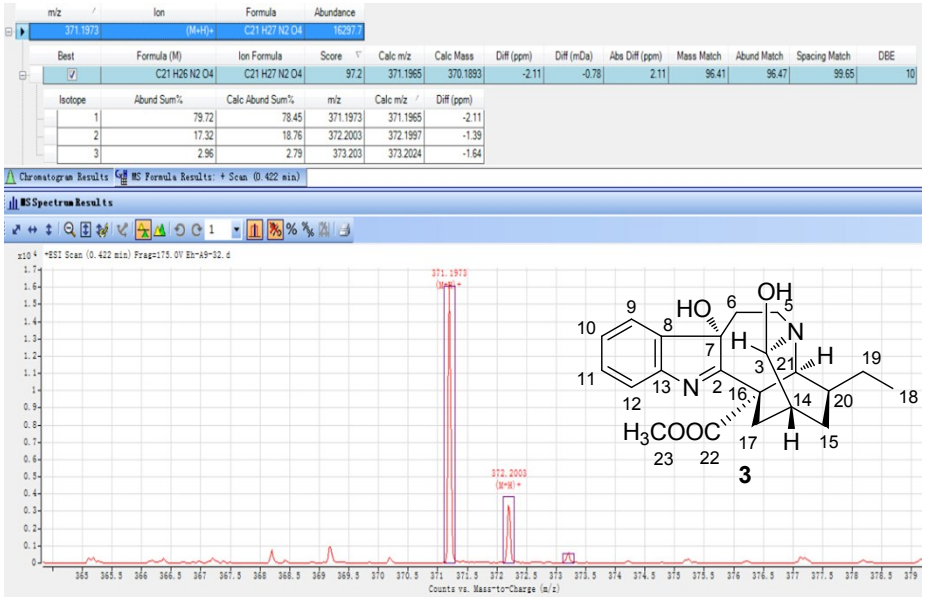

Fig. S31 HR-ESI-MS spectrum of **3**

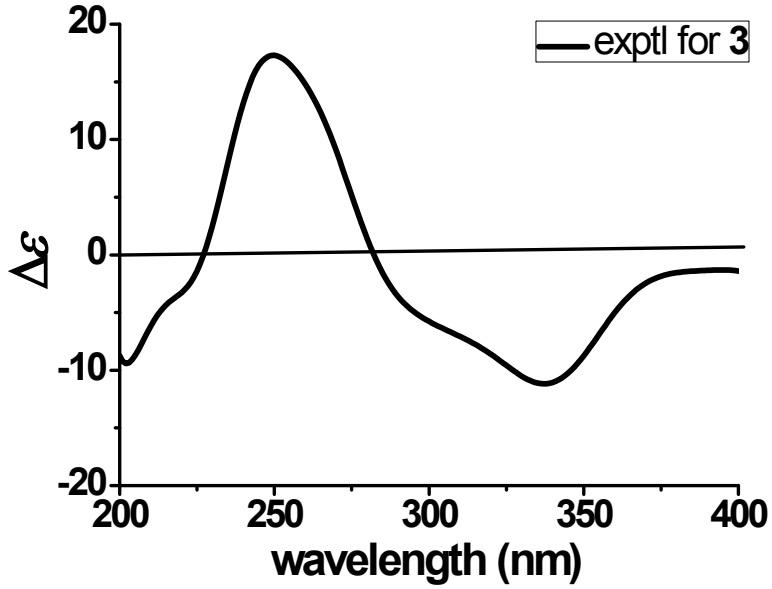

Fig. S32 ECD spectrum of **3** (CH_3CN)

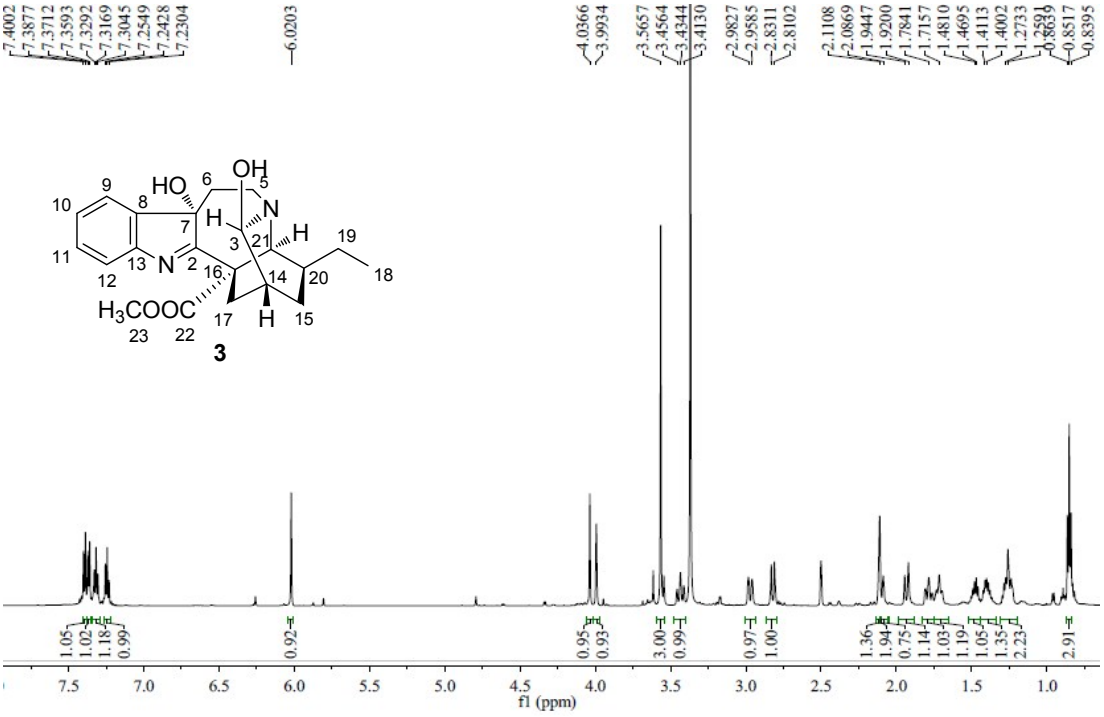

Fig. S33 ^{1}H-NMR spectrum of **3** (DMSO-d_6)

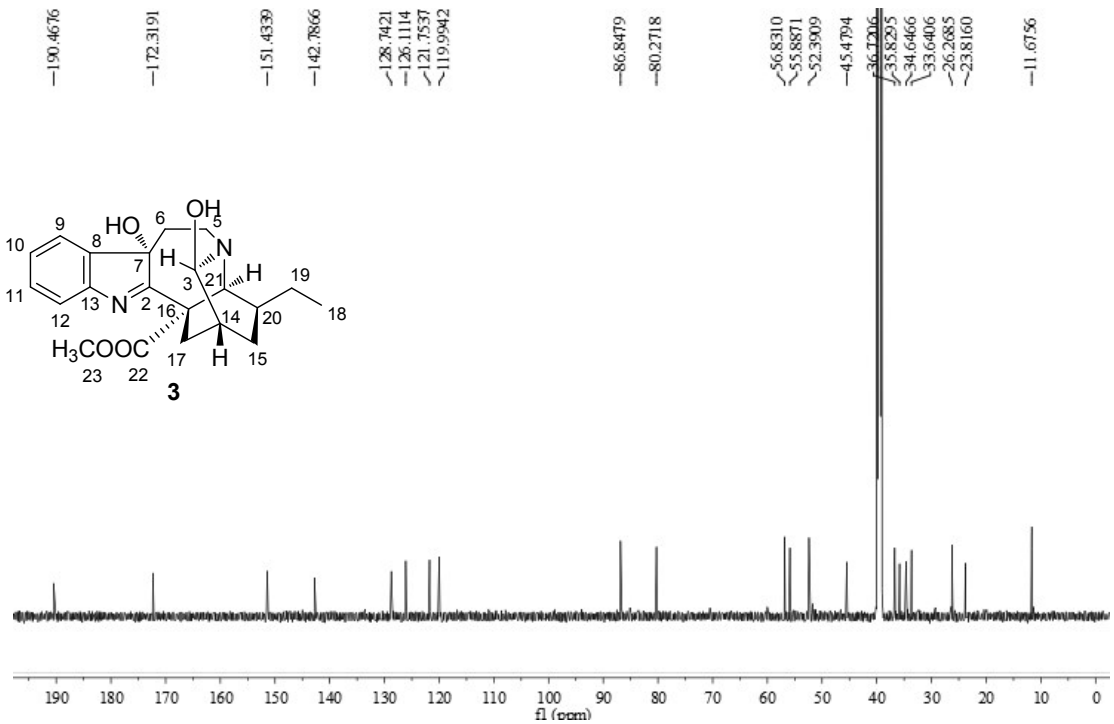

Fig. S34 ^{13}C-NMR spectrum of **3** (DMSO-d_6)

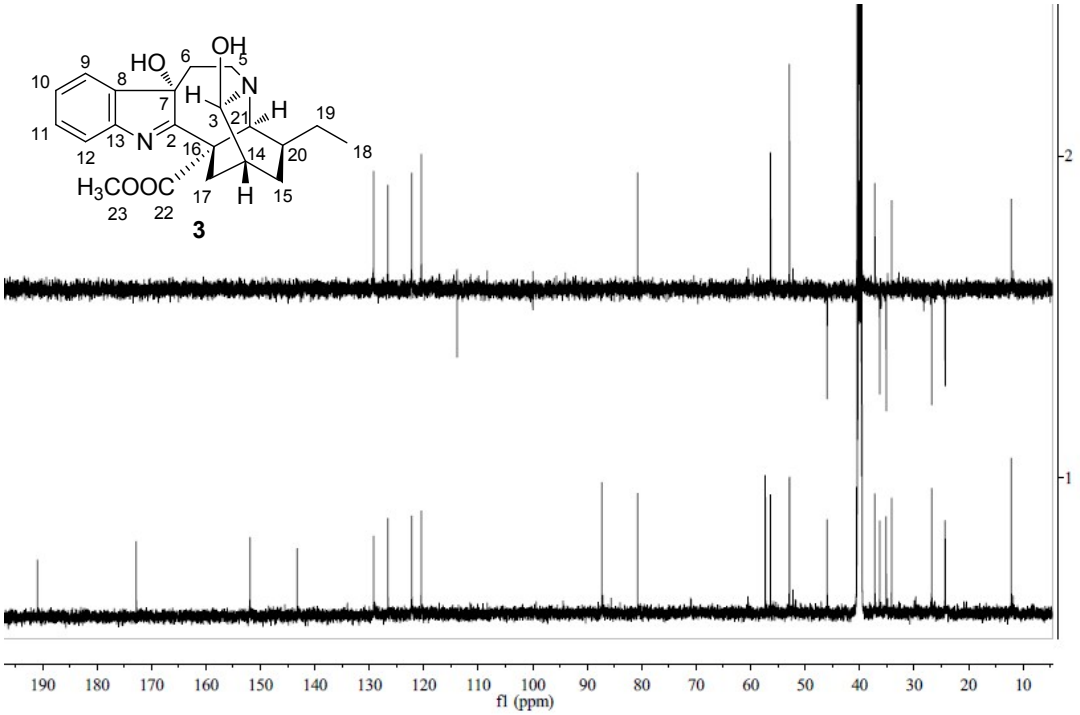

Fig. S35 DEPT-135 spectrum of **3** (DMSO-d_6)

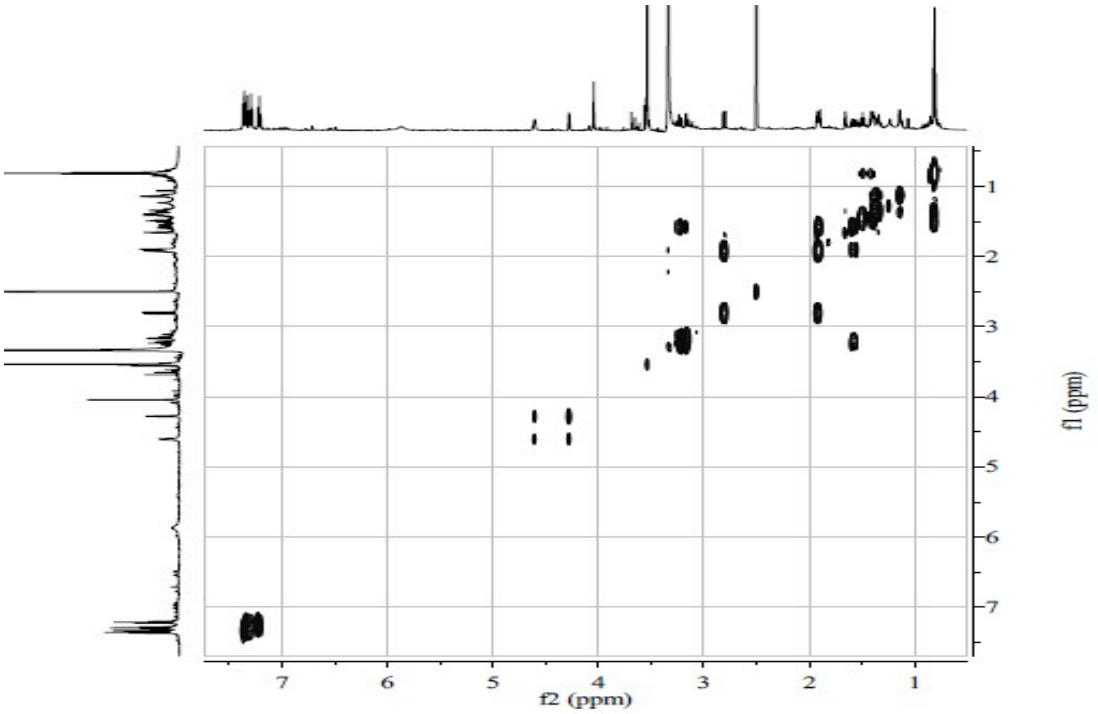

Fig. S36 ^{1}H-^{1}H COSY spectrum of **3** (DMSO-d_6)

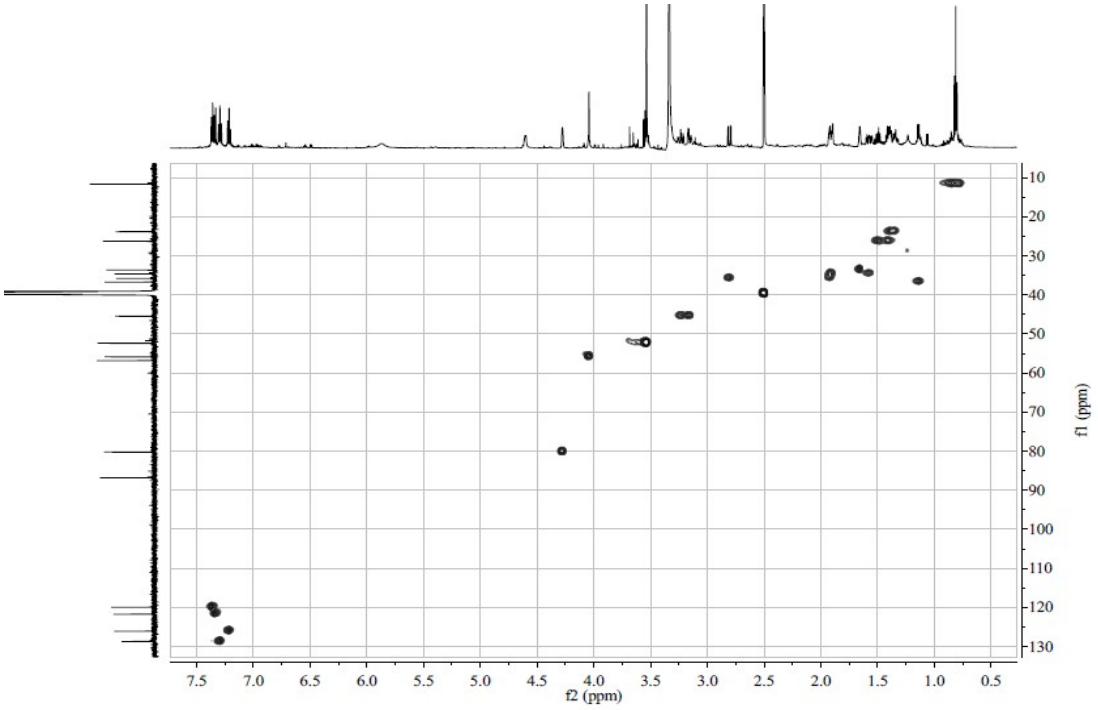

Fig. S37 HSQC spectrum of **3** (DMSO-d_6)

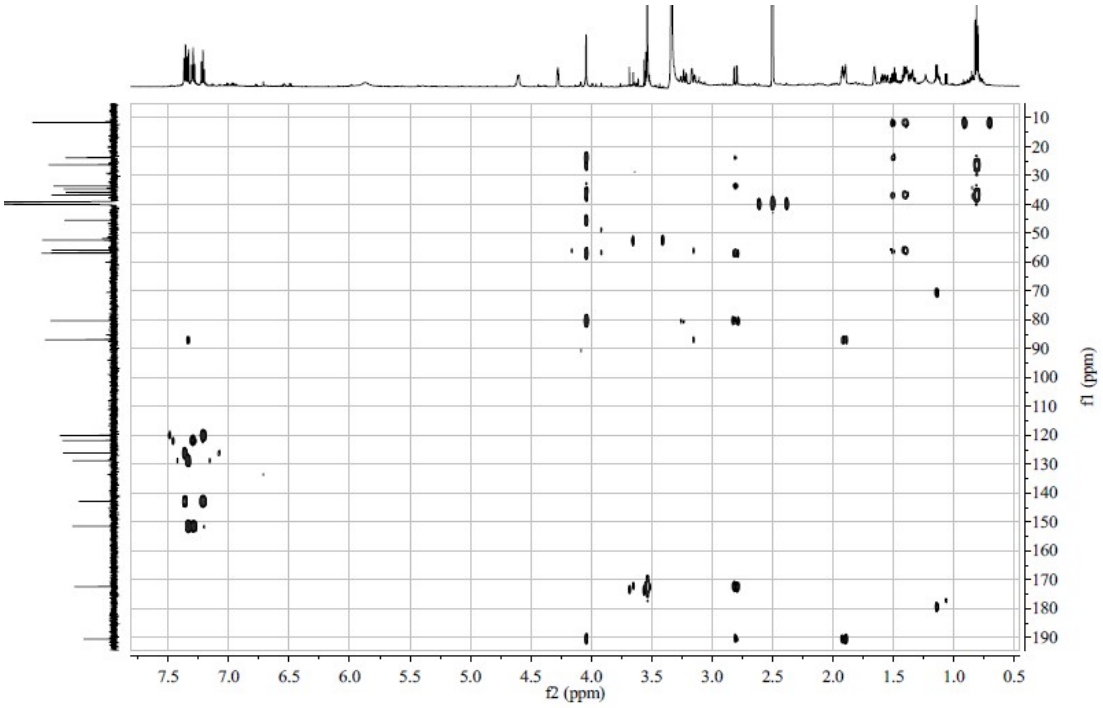

Fig. S38 HMBC spectrum of **3** (DMSO-d_6)

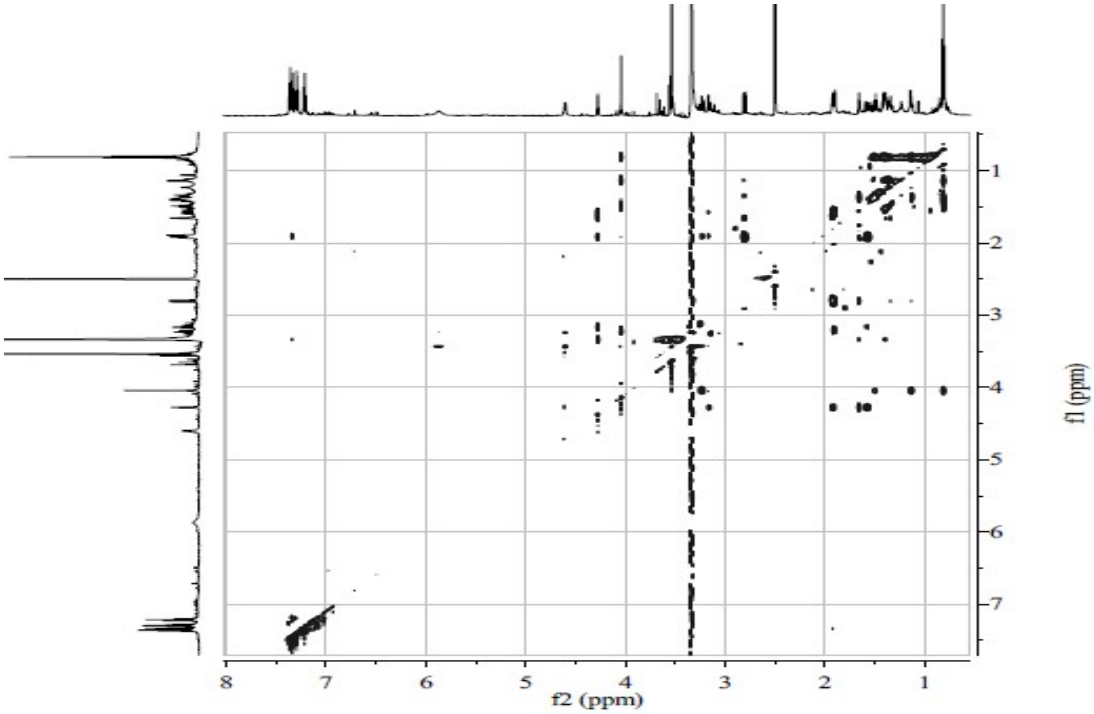

Fig. S39 NOESY spectrum of **3** (DMSO-d_6)

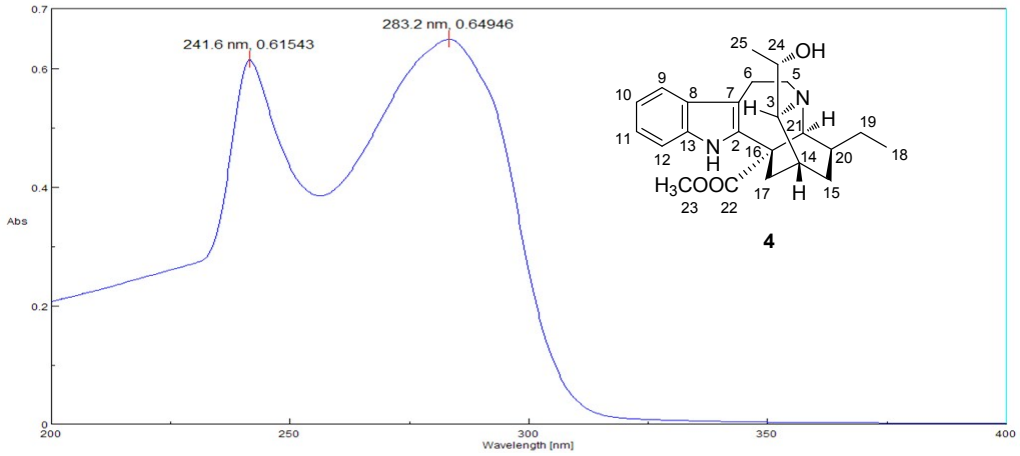

Fig. S40 UV spectrum of **4** ($CHCl_3$)

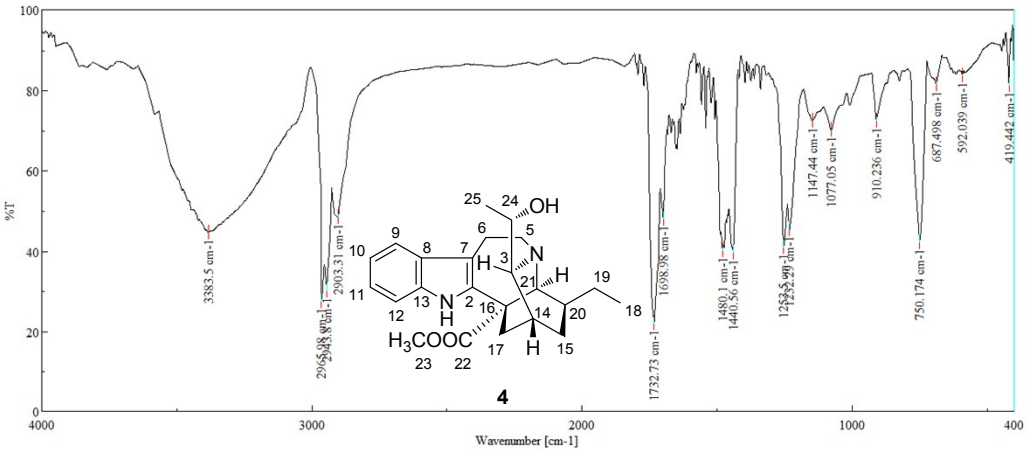

Fig. S41 IR spectrum of **4** (KBr)

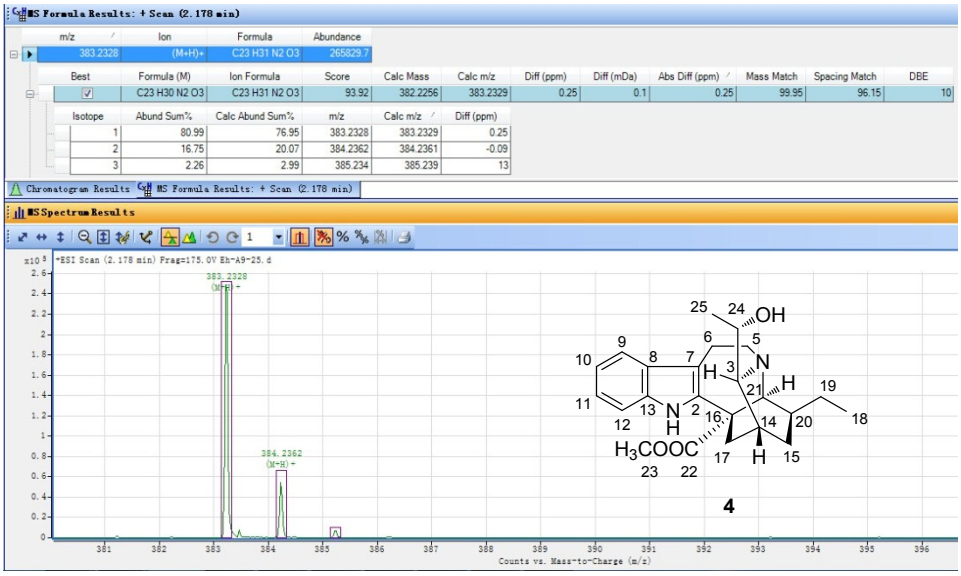

Fig. S42 HRESIMS spectrum of **4**

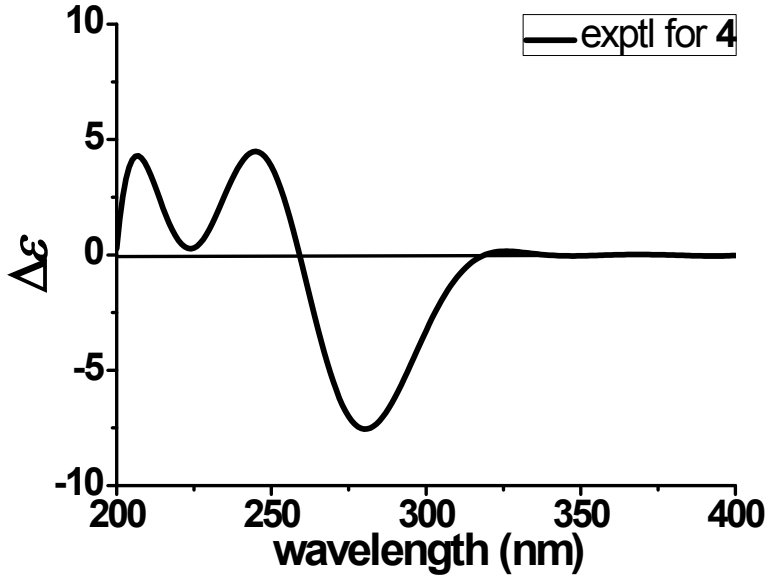

Fig. S43 CD spectrum of **4** (CH_3CN)

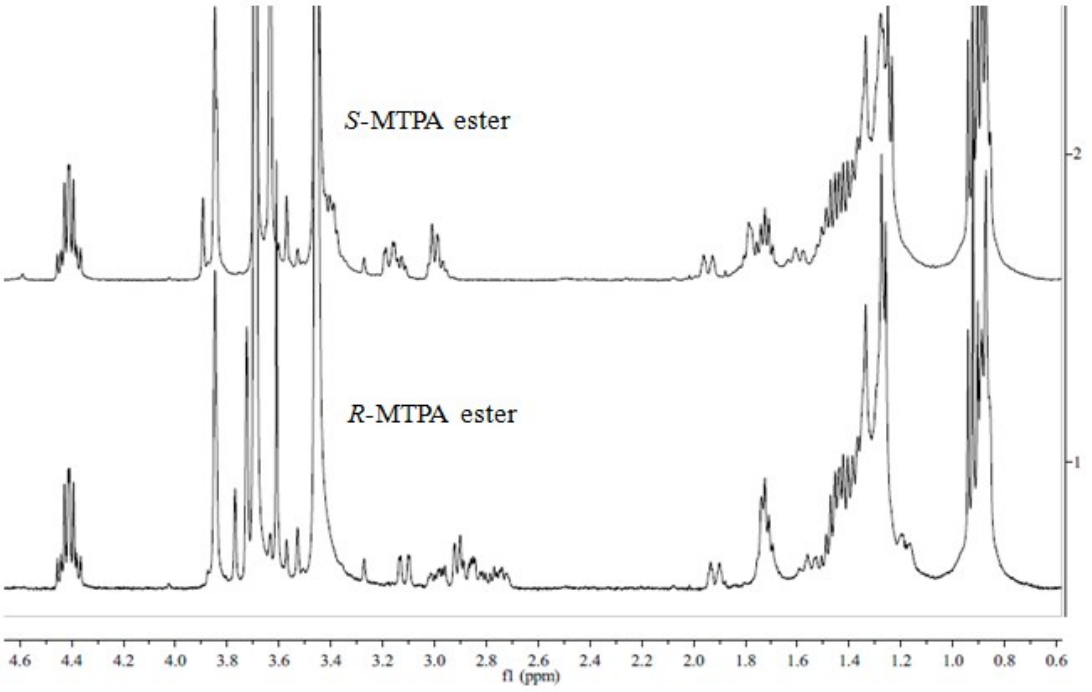

Fig. S44 ^{1}H-NMR spectrum of (*S*)-MTPA ester and (*R*)-MTPA ester of **4** (pyridine-d_5)

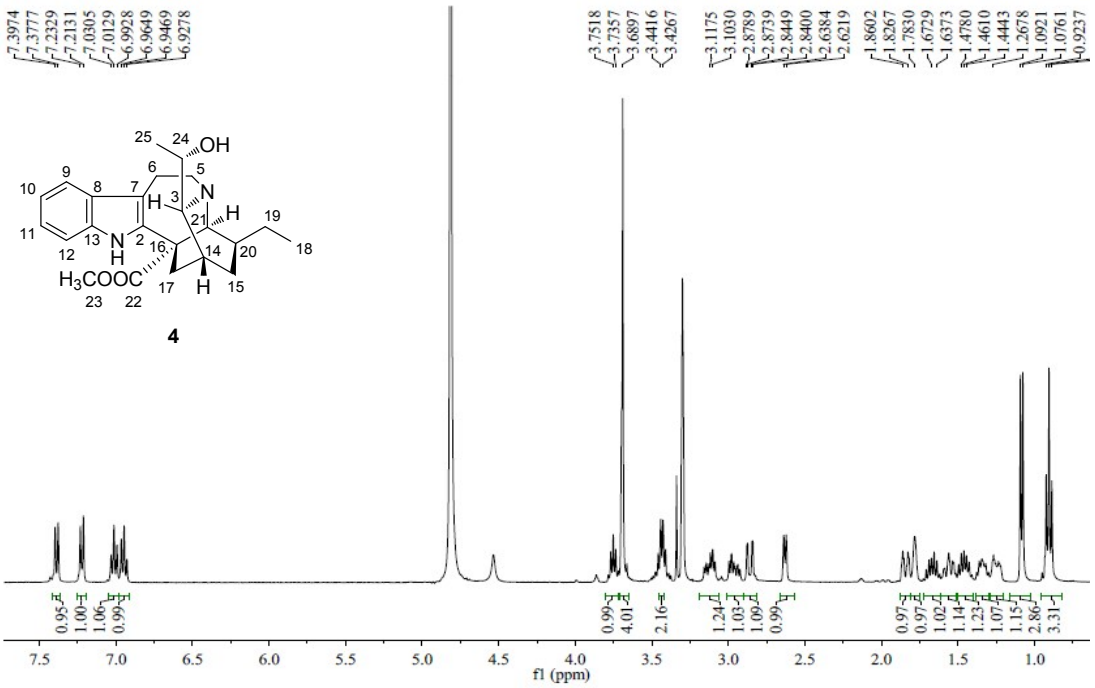

4

Fig. S45 ^{1}H-NMR spectrum of **4** (CD_3OD)

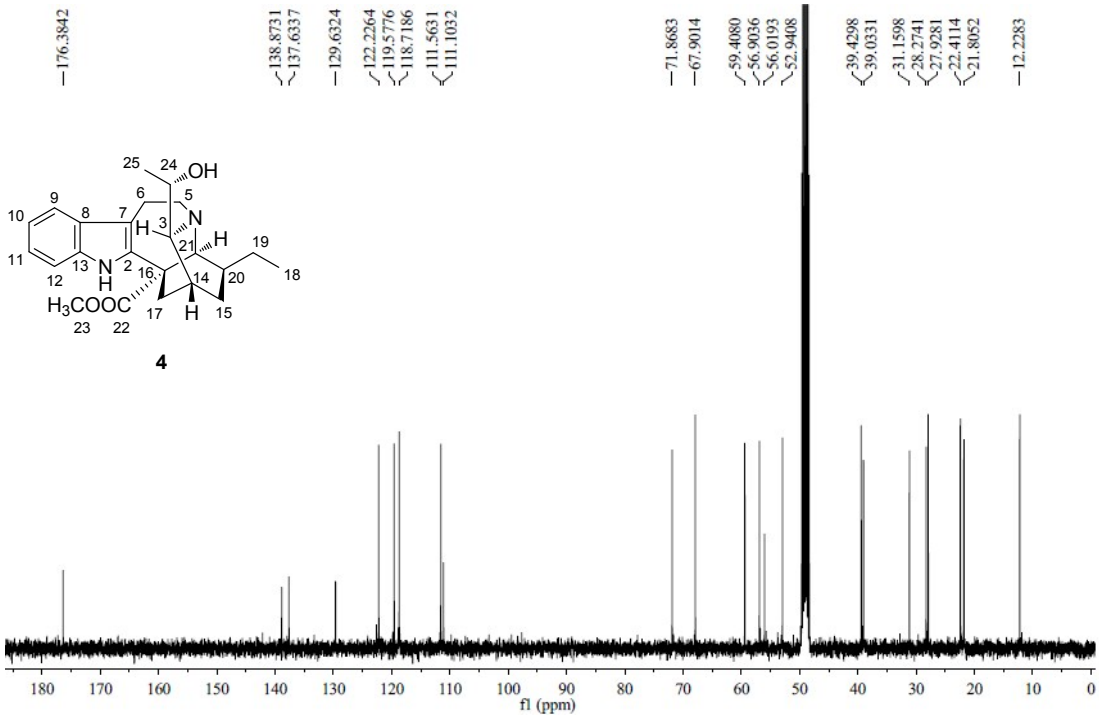

4

Fig. S46 ^{13}C-NMR spectrum of **4** (CD_3OD)

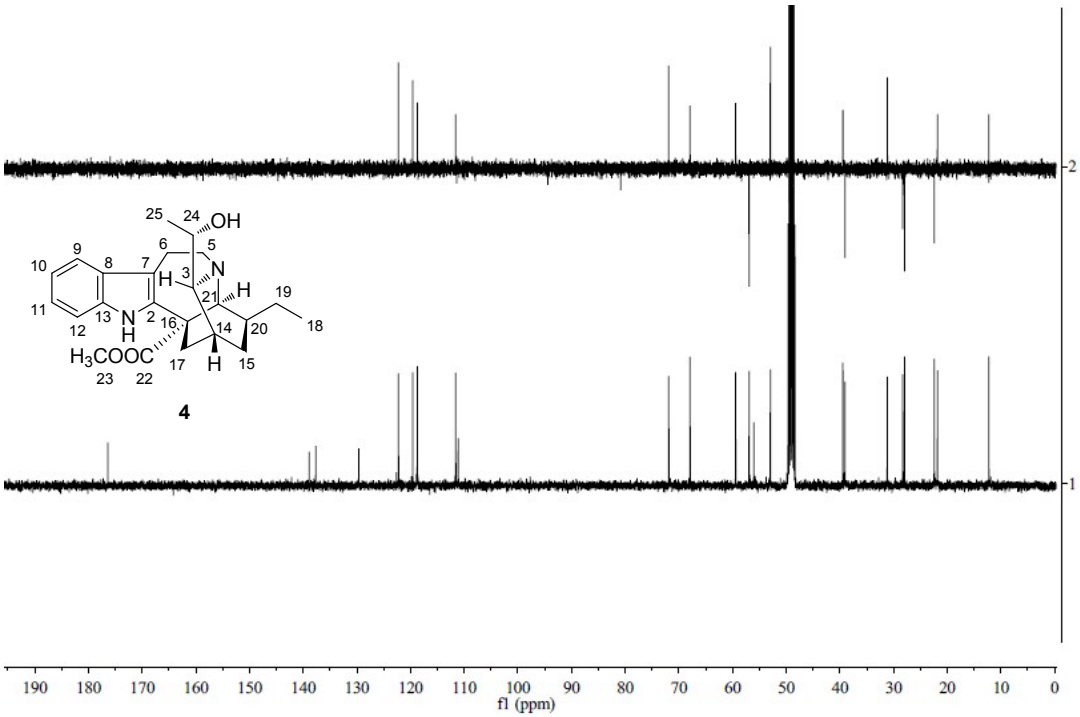

Fig. S47 DEPT-135 spectrum of **4** (CD_3OD)

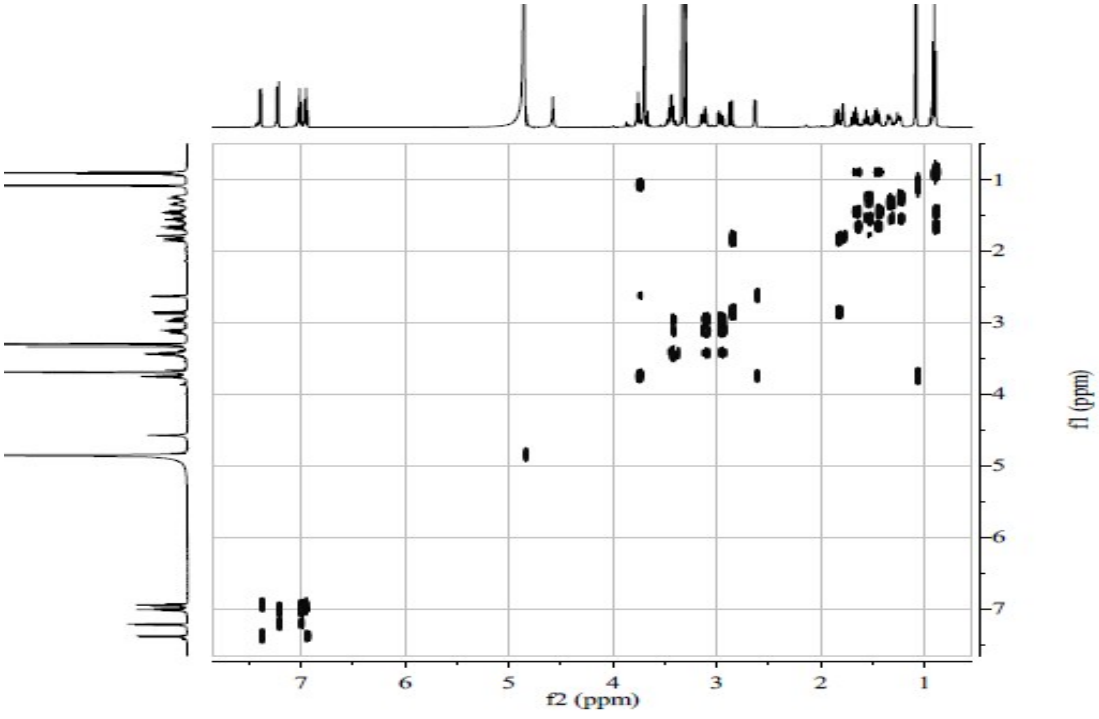

Fig. S48 ^{1}H-^{1}H COSY spectrum of **4** (CD_3OD)

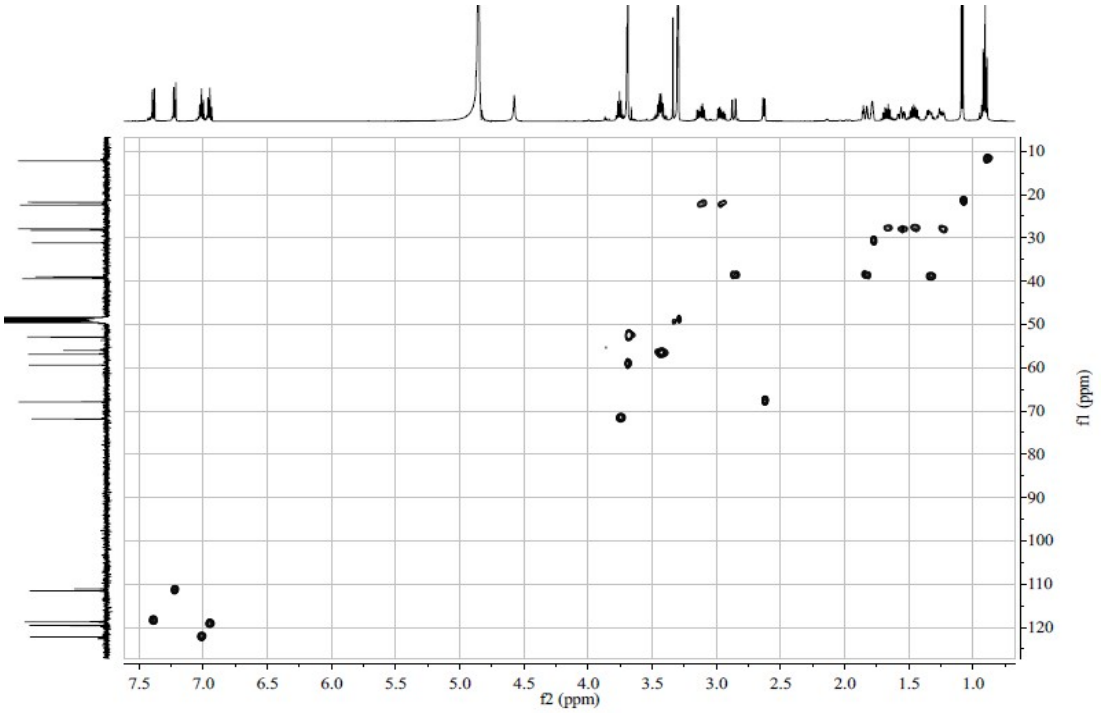

Fig. S49 HSQC spectrum of **4** (CD_3OD)

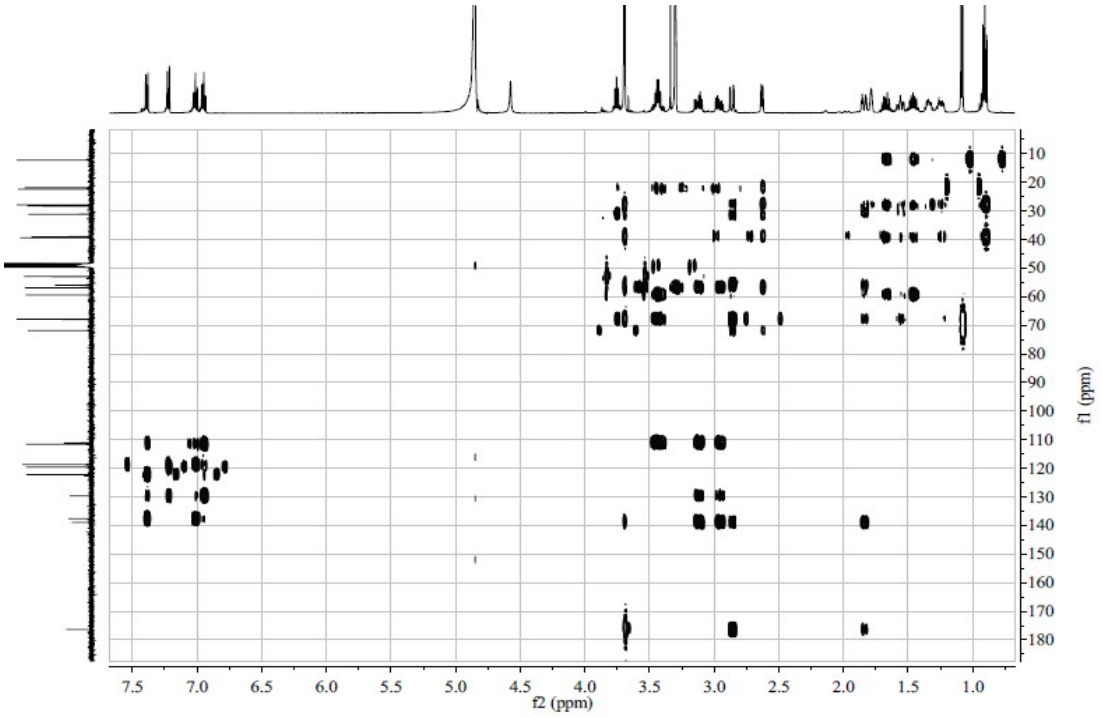

Fig. S50 HMBC spectrum of **4** (CD_3OD)

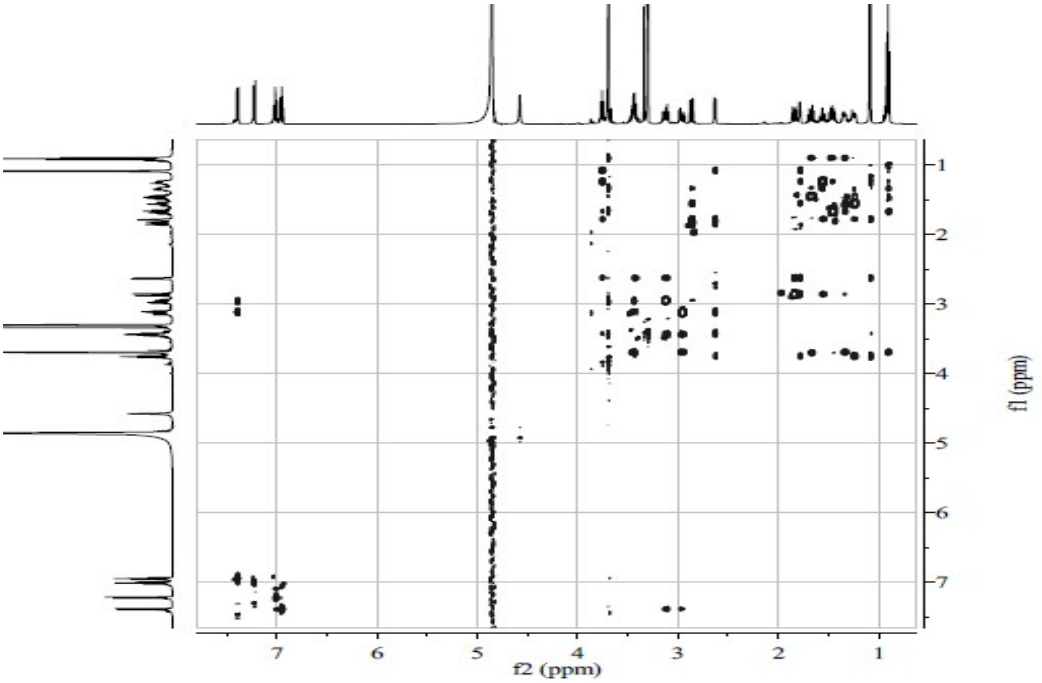

Fig. S51 NOESY spectrum of **4** (CD_3OD)

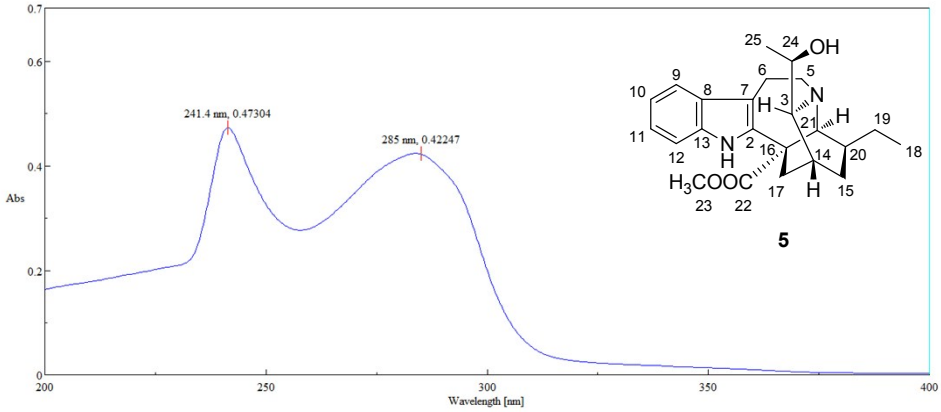

Fig. S52 UV spectrum of **5** ($CHCl_3$)

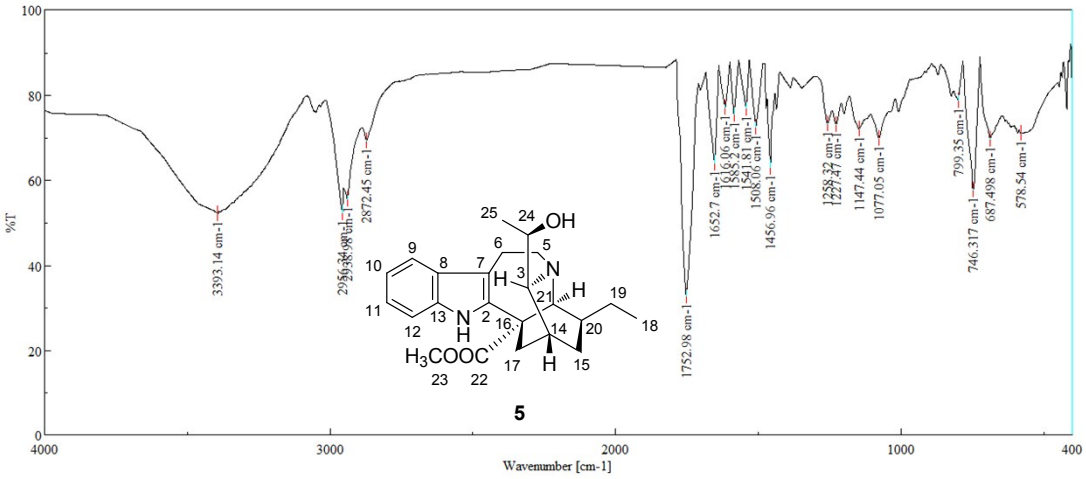

Fig. S53 IR spectrum of **5** (KBr)

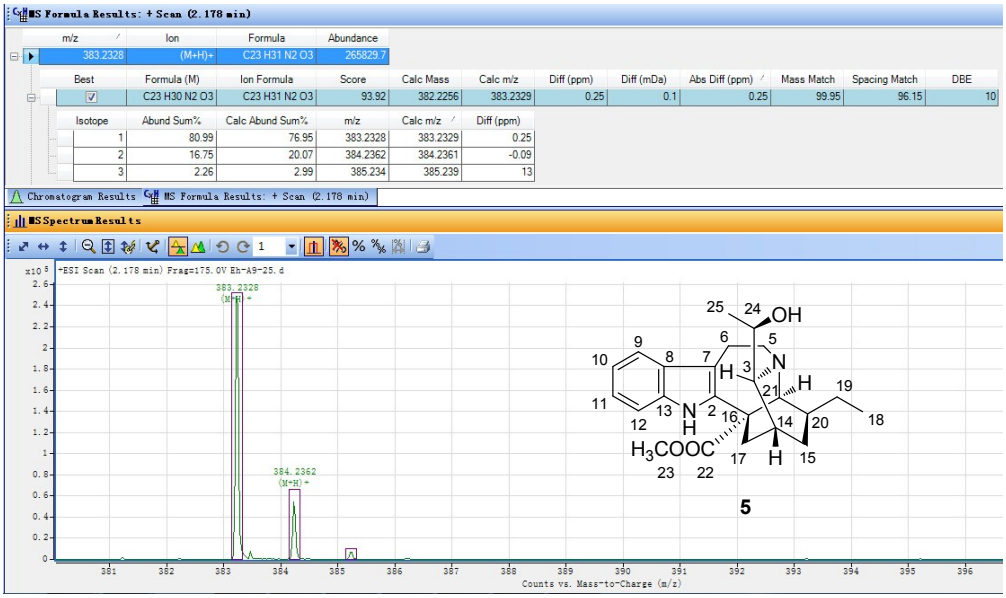

Fig. S54 HR-ESI-MS spectrum of **5**

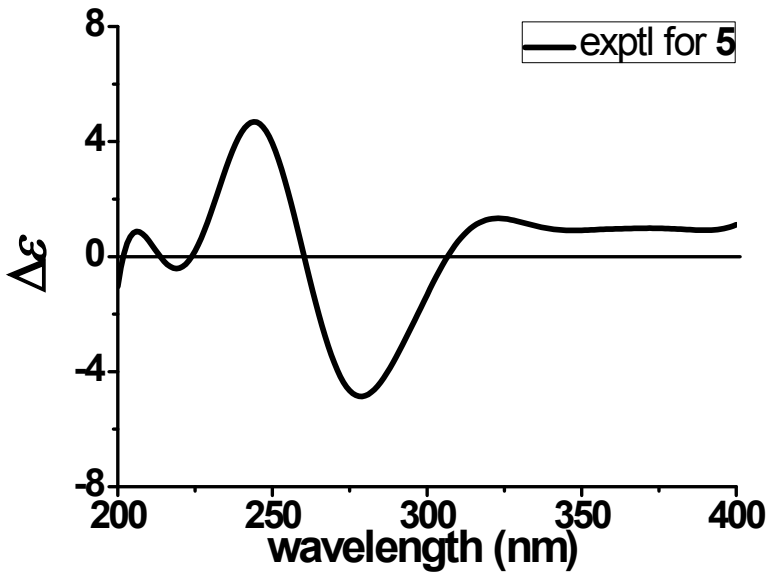

Fig. S55 CD spectrum of **5** (CH_3CN)

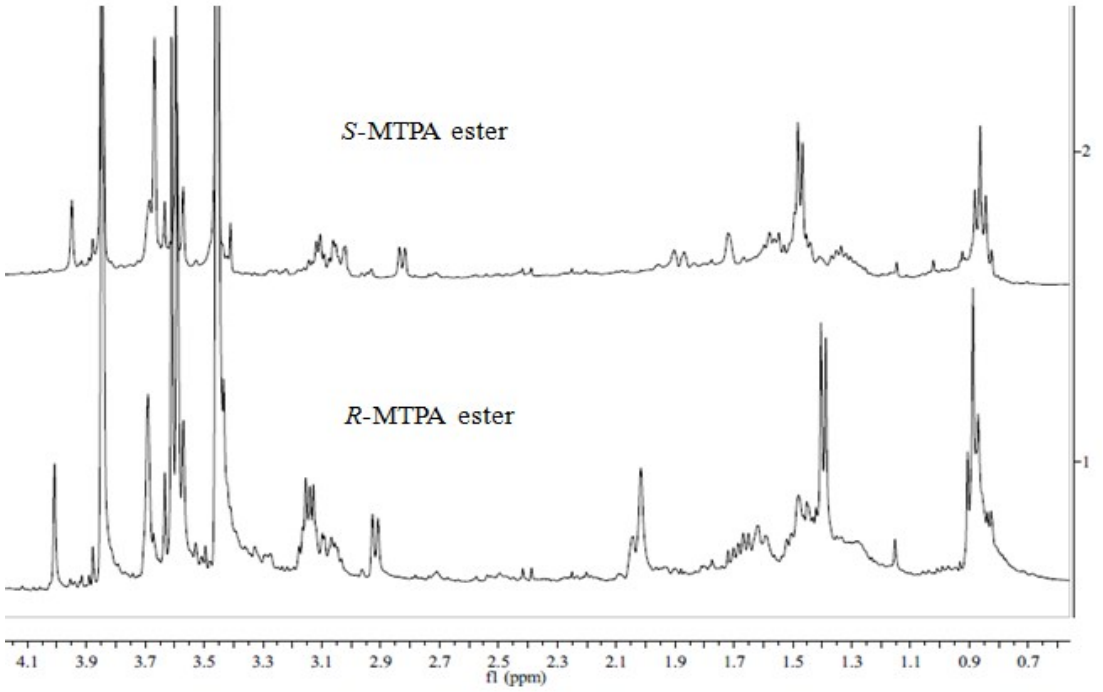

Fig. S56 ^{1}H-NMR spectrum of (*S*)-MTPA ester and (*R*)-MTPA ester of **5** (pyridine-d_5)

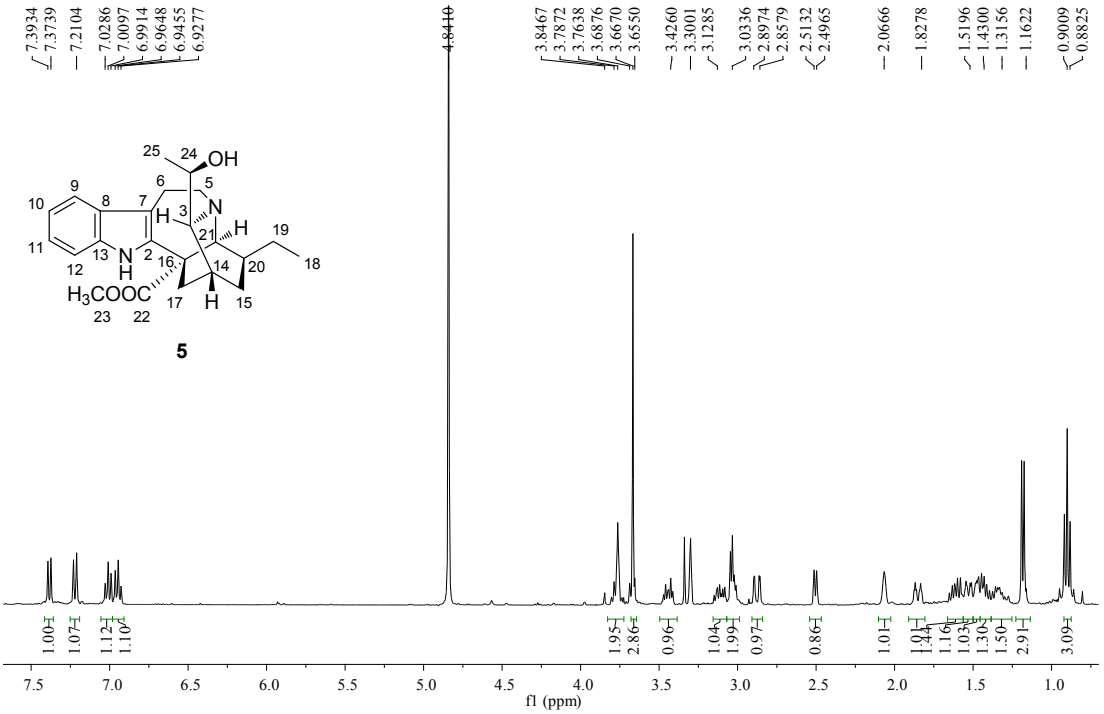

Fig. S57 ^{1}H-NMR spectrum of **5** (CD_3OD)

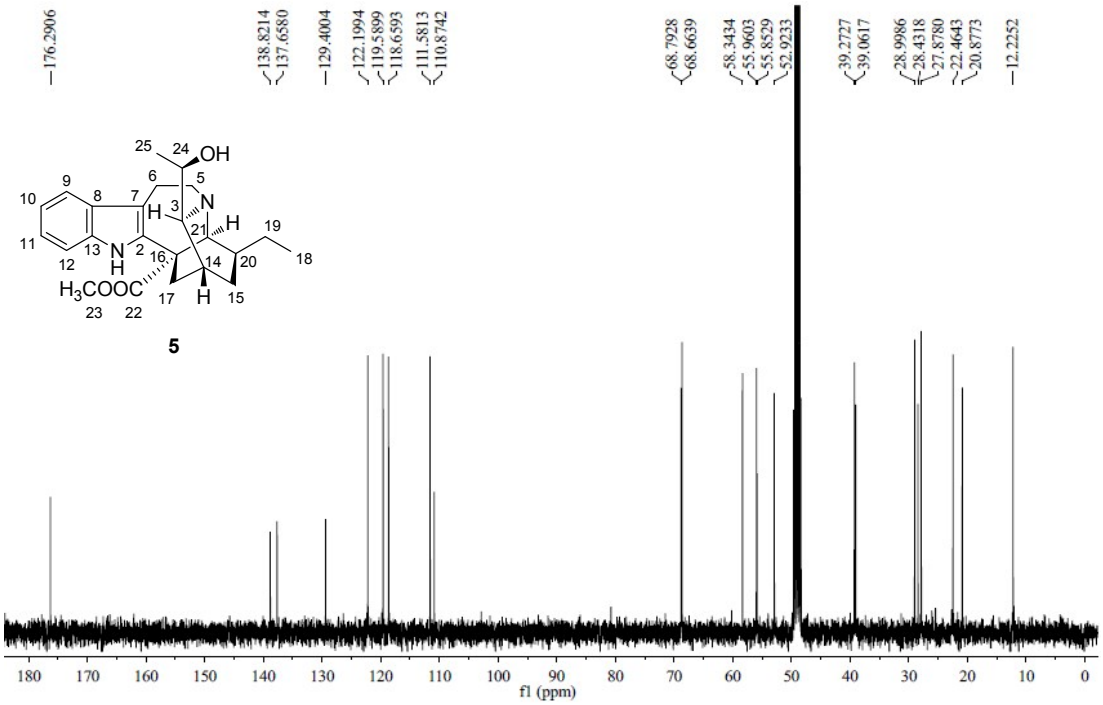

Fig. S58 ^{13}C-NMR spectrum of **5** (CD_3OD)

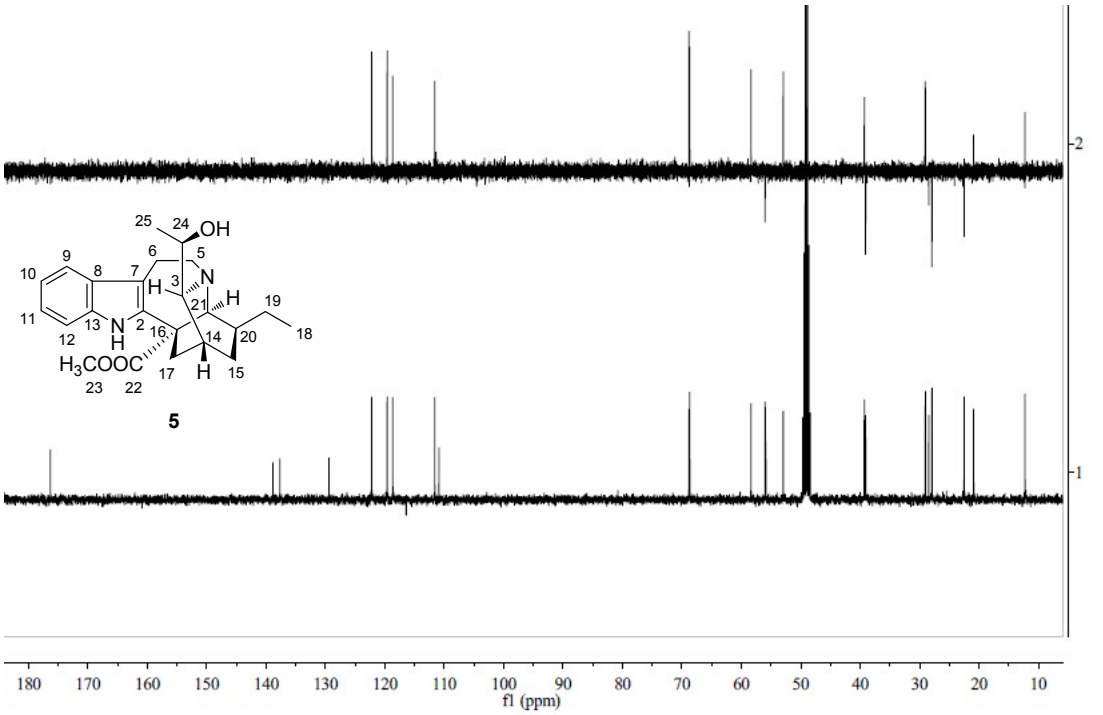

Fig. S59 DEPT-135 spectrum of **5** (CD_3OD)

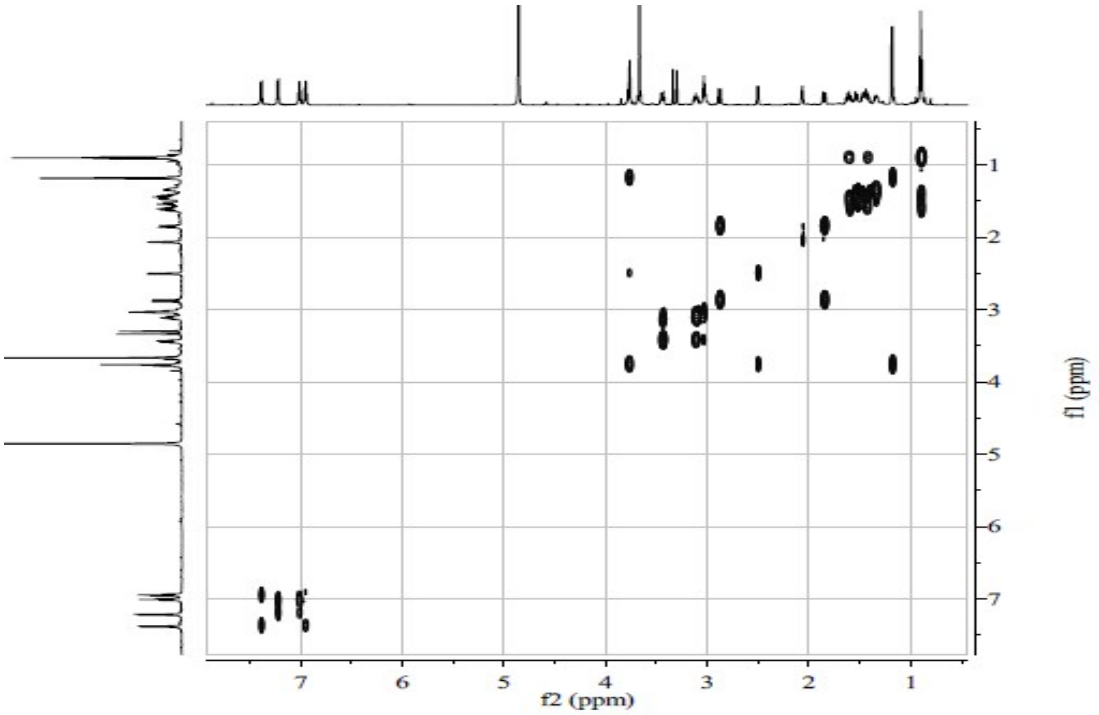

Fig. S60 ^{1}H-^{1}H COSY spectrum of **5** (CD_3OD)

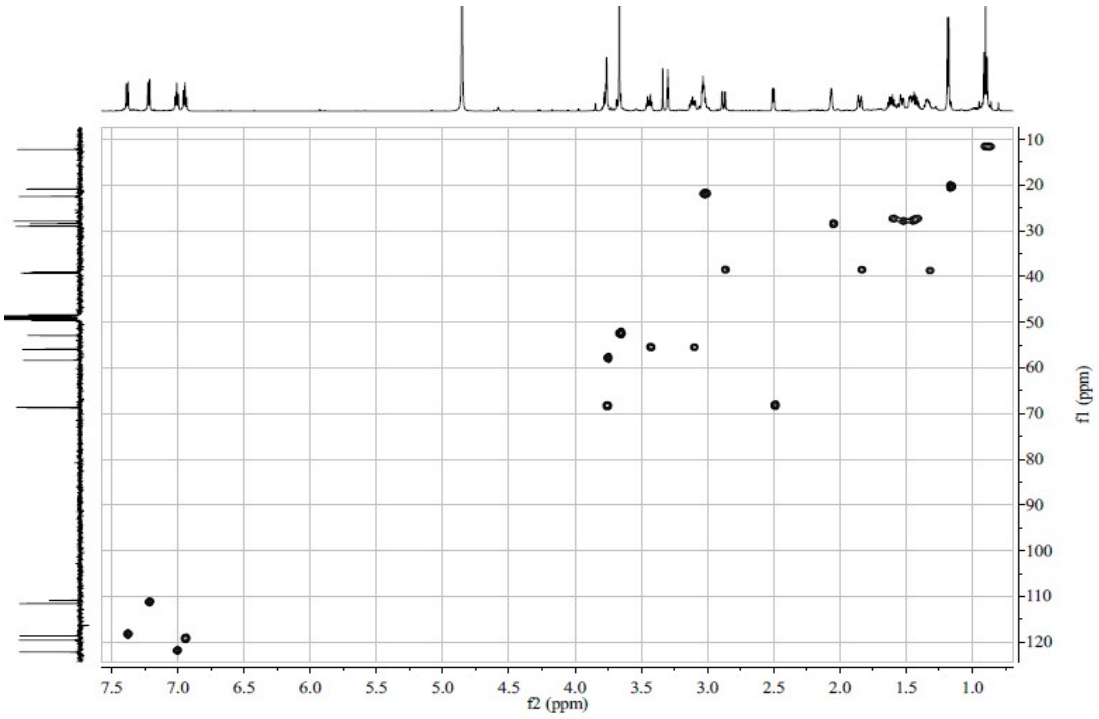

Fig. S61 HSQC spectrum of **5** (CD_3OD)

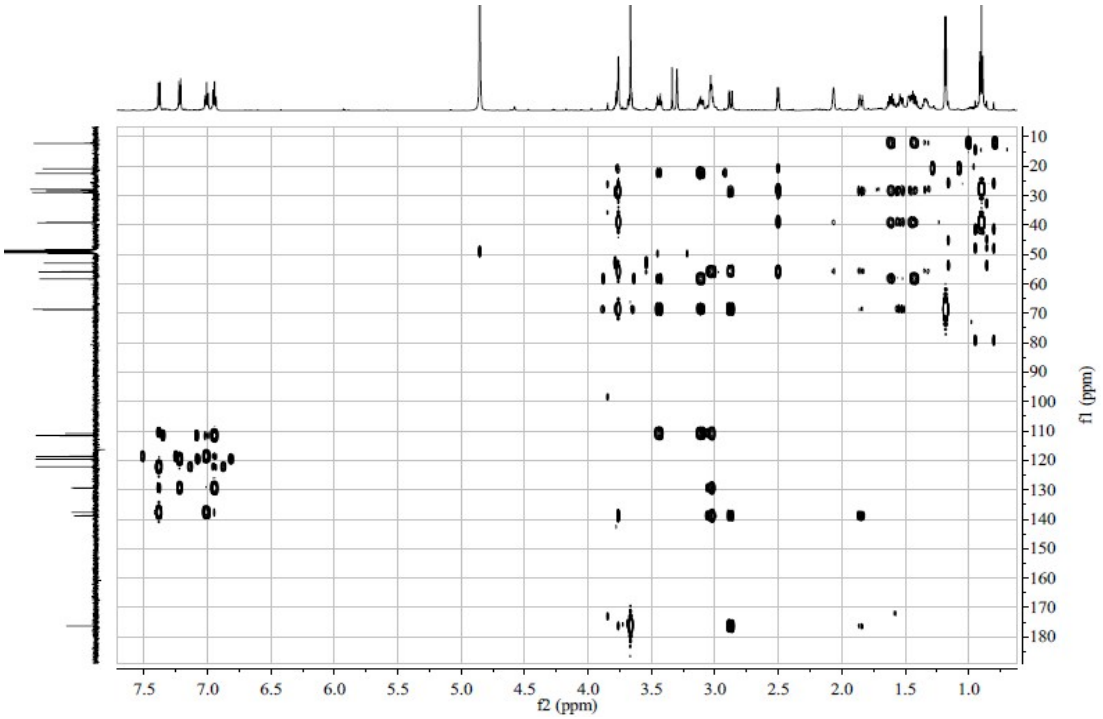

Fig. S62 HMBC spectrum of **5** (CD_3OD)

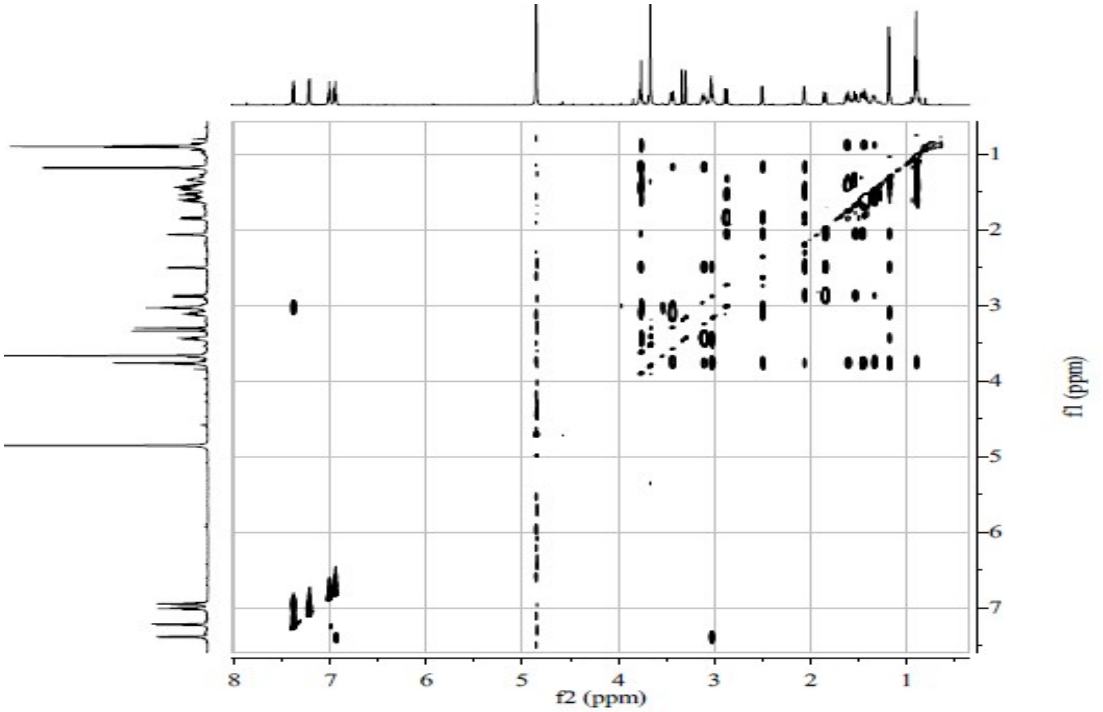

Fig. S63 NOESY spectrum of **5** (CD_3OD)

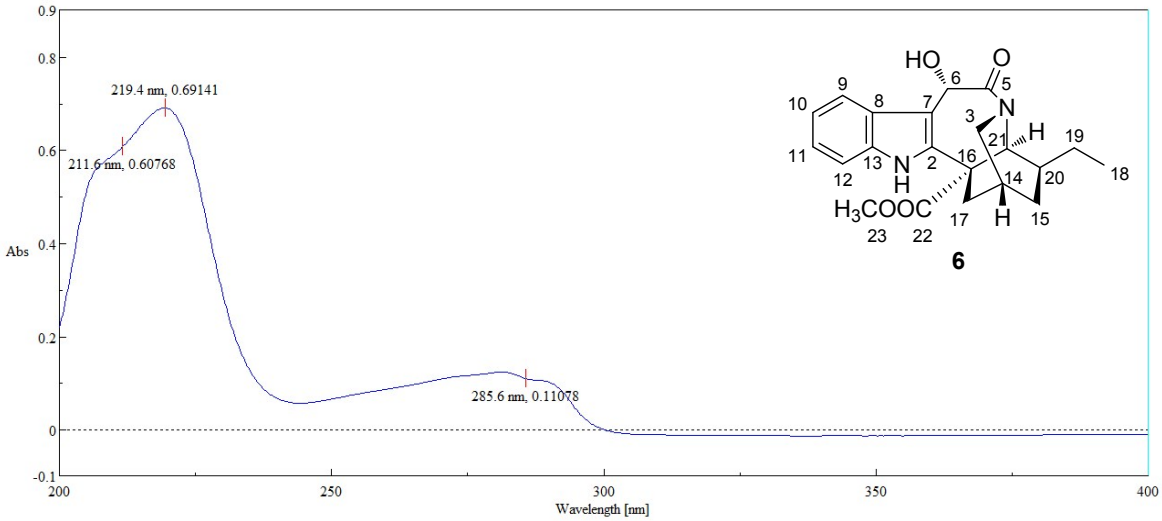

Fig. S64 UV spectrum of **6** ($CHCl_3$)

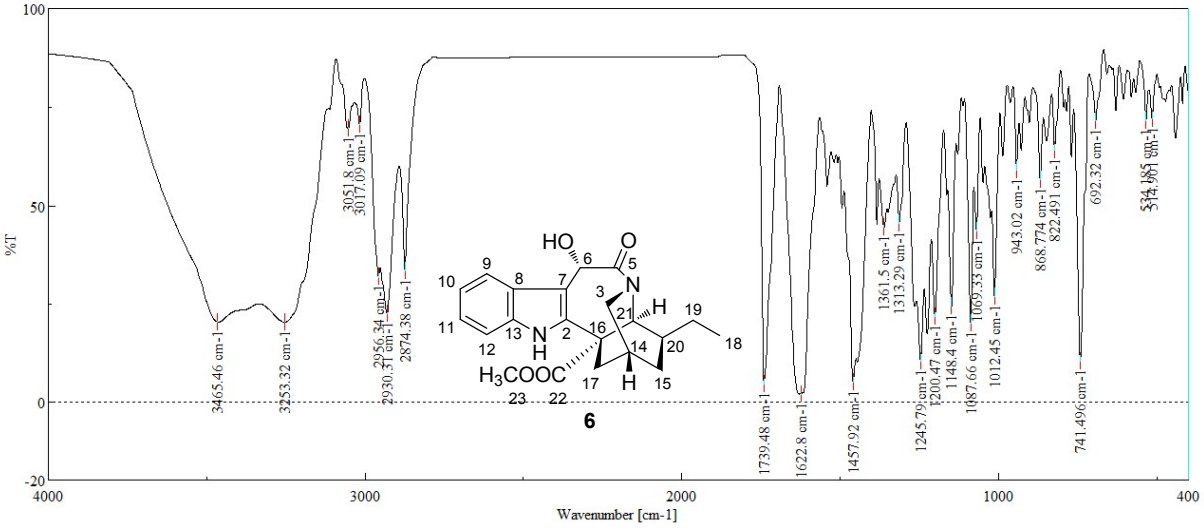

Fig. S65 IR spectrum of **6** (KBr)

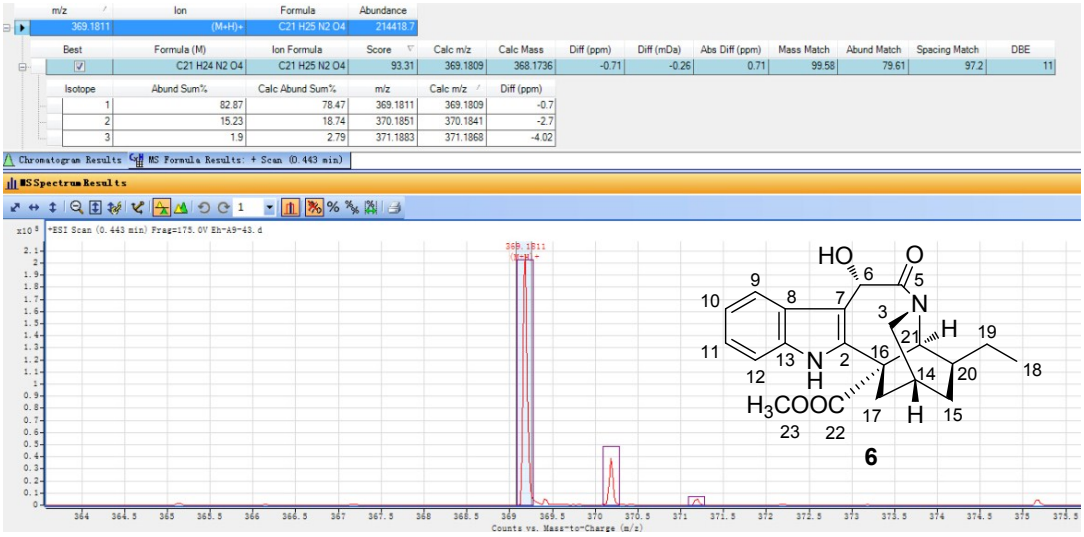

Fig. S66 HR-ESI-MS spectrum of **6**

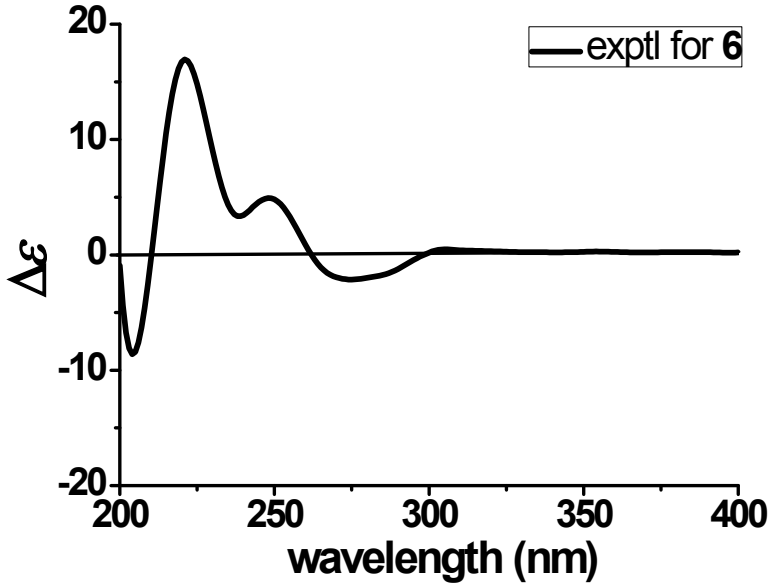

Fig. S67 CD spectrum of **6** (CH_3CN)

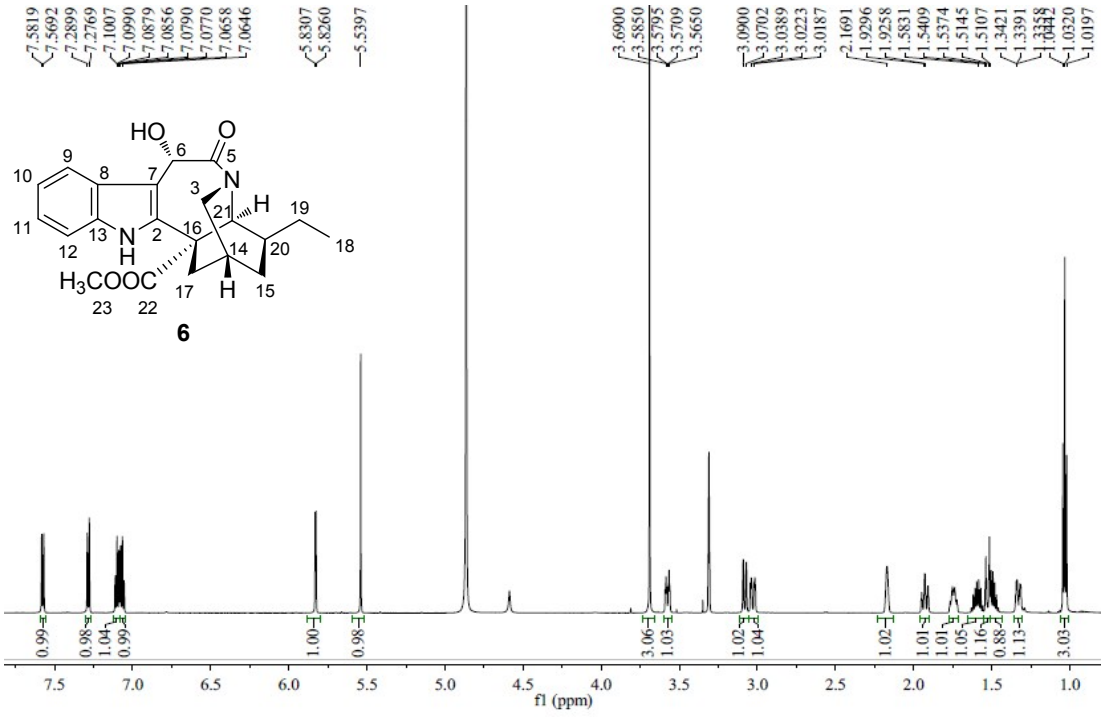

Fig. S68 ^{1}H-NMR spectrum of **6** (CD_3OD)

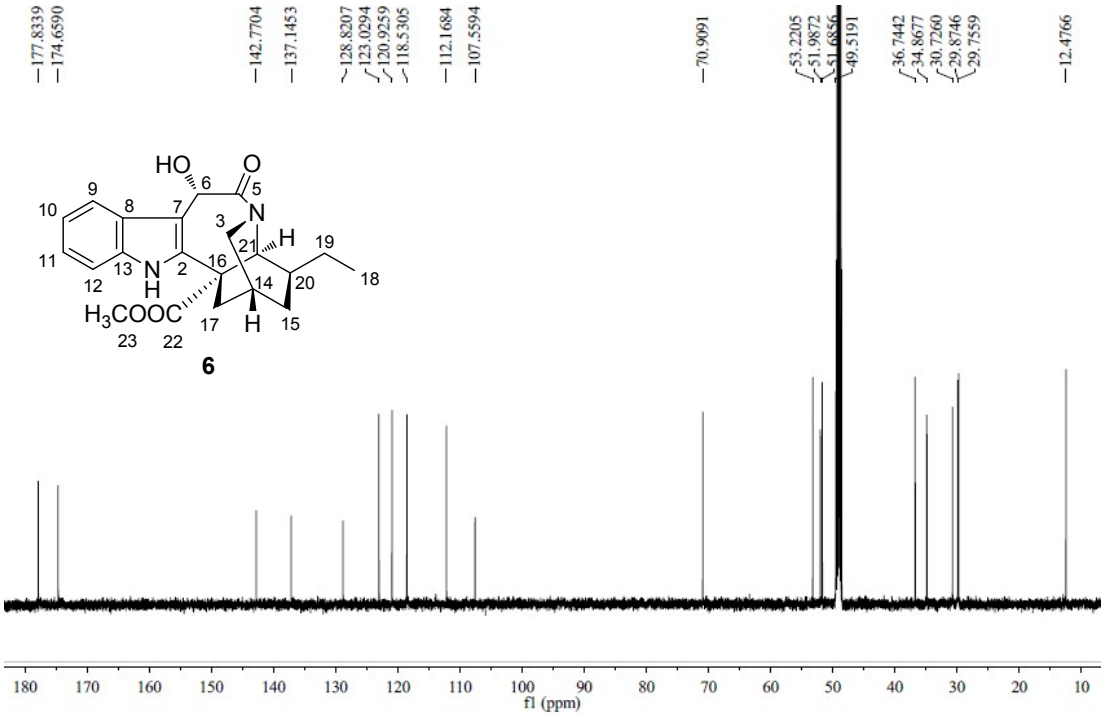

Fig. S69 ^{13}C-NMR spectrum of **6** (CD_3OD)

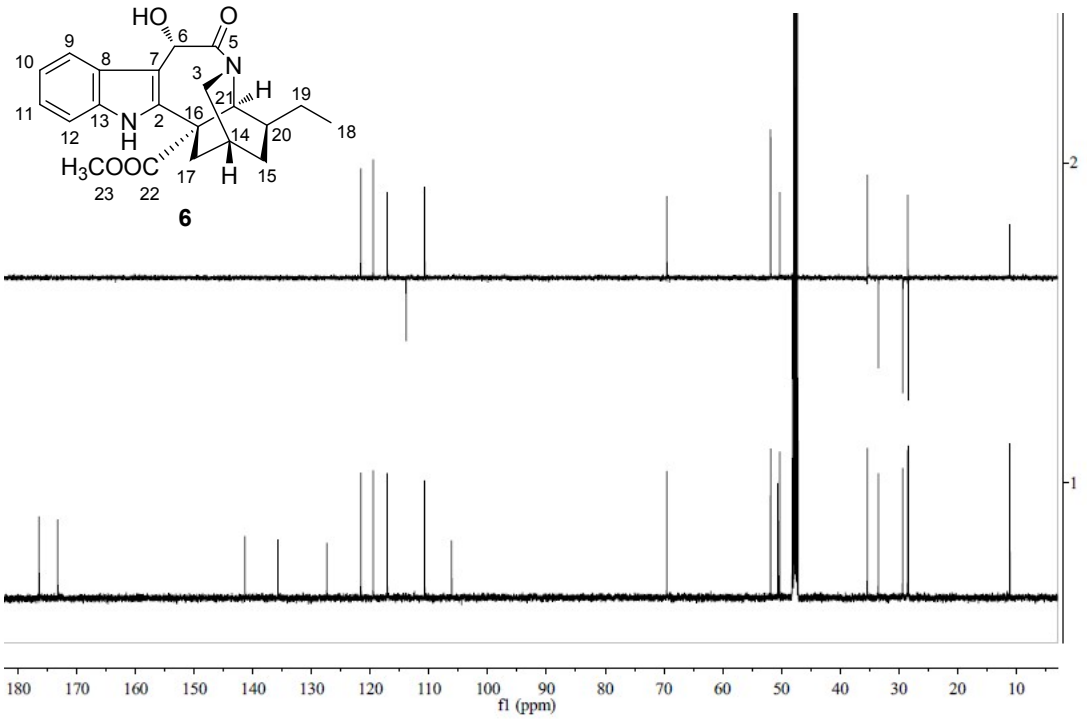

Fig. S70 DEPT-135 spectrum of **6** (CD_3OD)

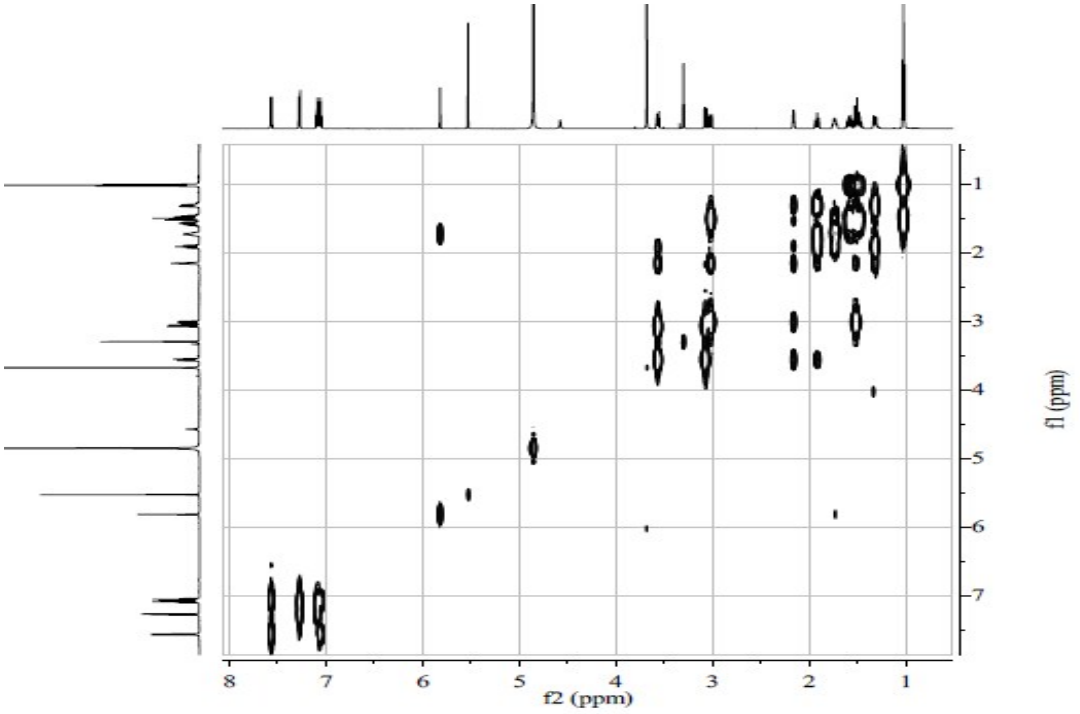

Fig. S71 ^{1}H-^{1}H COSY spectrum of **6** (CD_3OD)

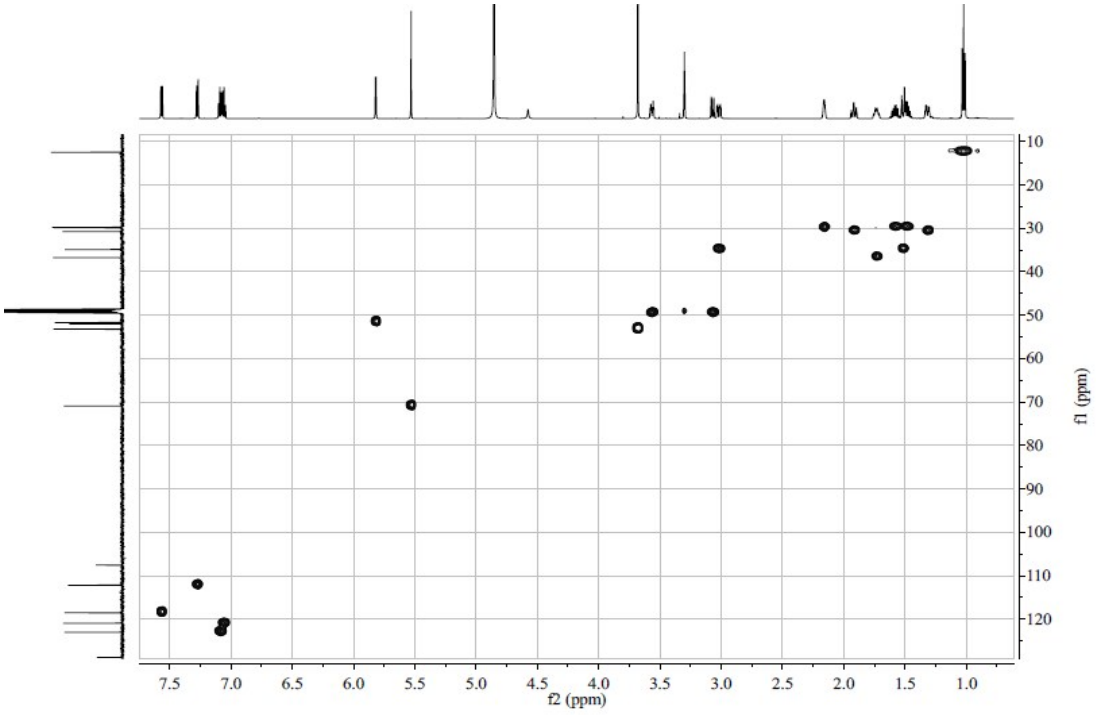

Fig. S72 HSQC spectrum of **6** (CD_3OD)

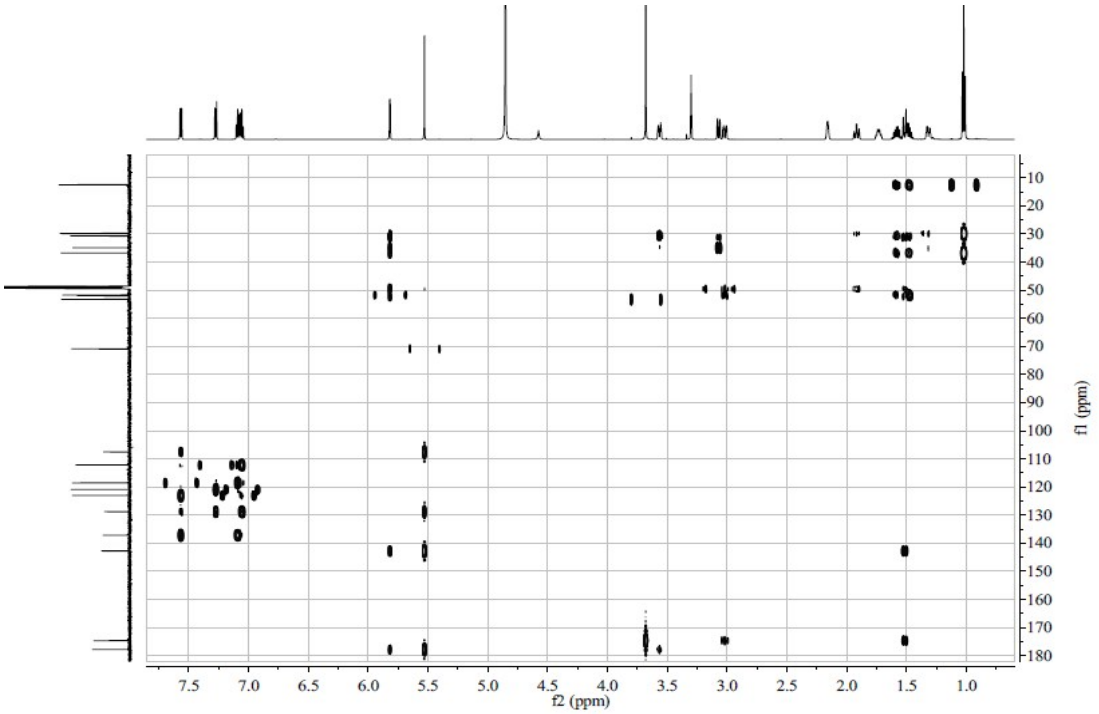

Fig. S73 HMBC spectrum of **6** (CD_3OD)

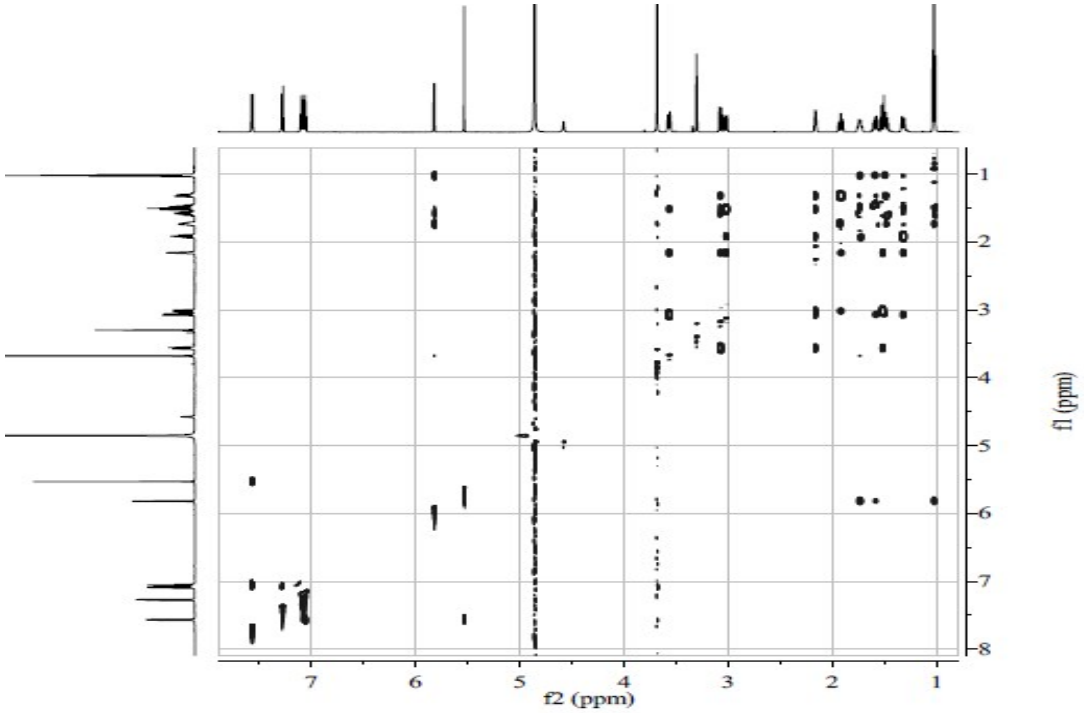

Fig. S74 NOESY spectrum of **6** (CD_3OD)

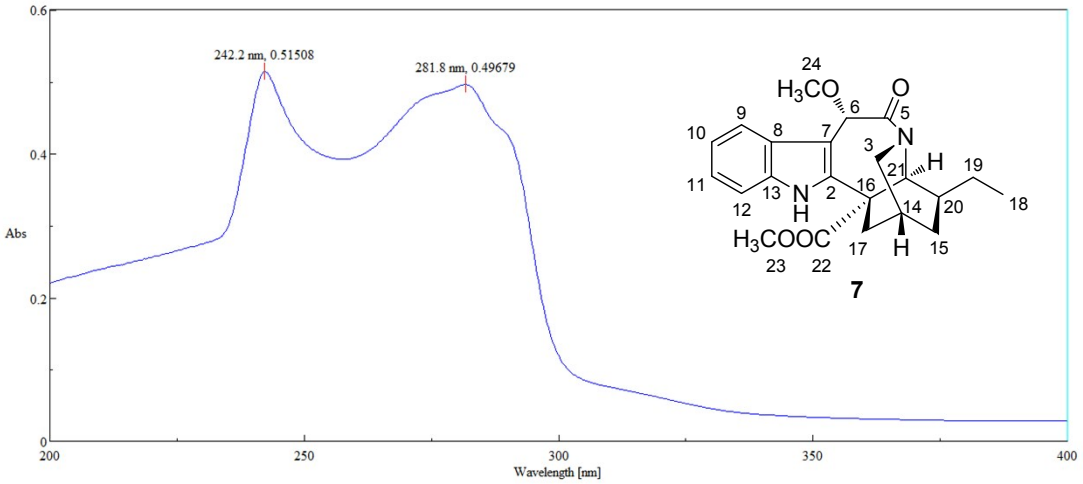

Fig. S75 UV spectrum of **7** ($CHCl_3$)

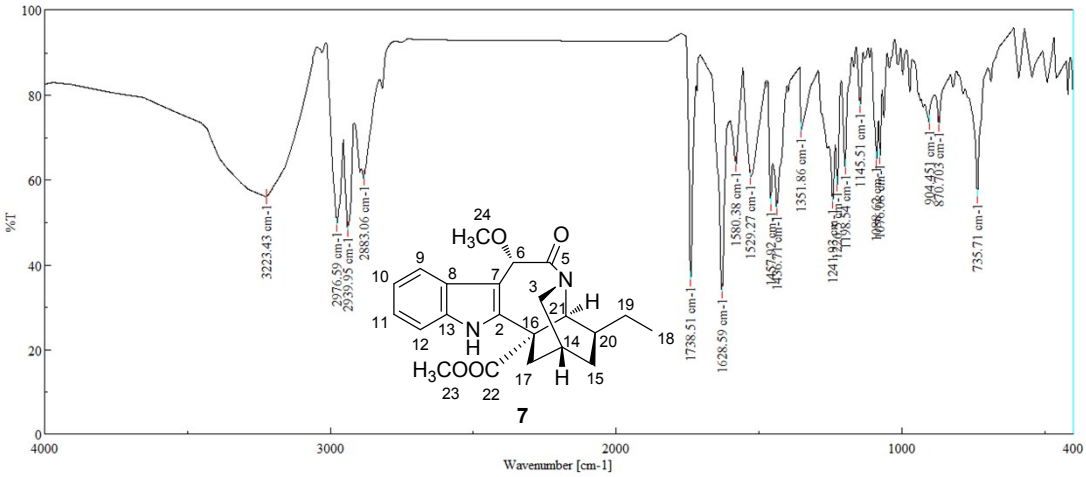

Fig. S76 IR spectrum of **7** (KBr)

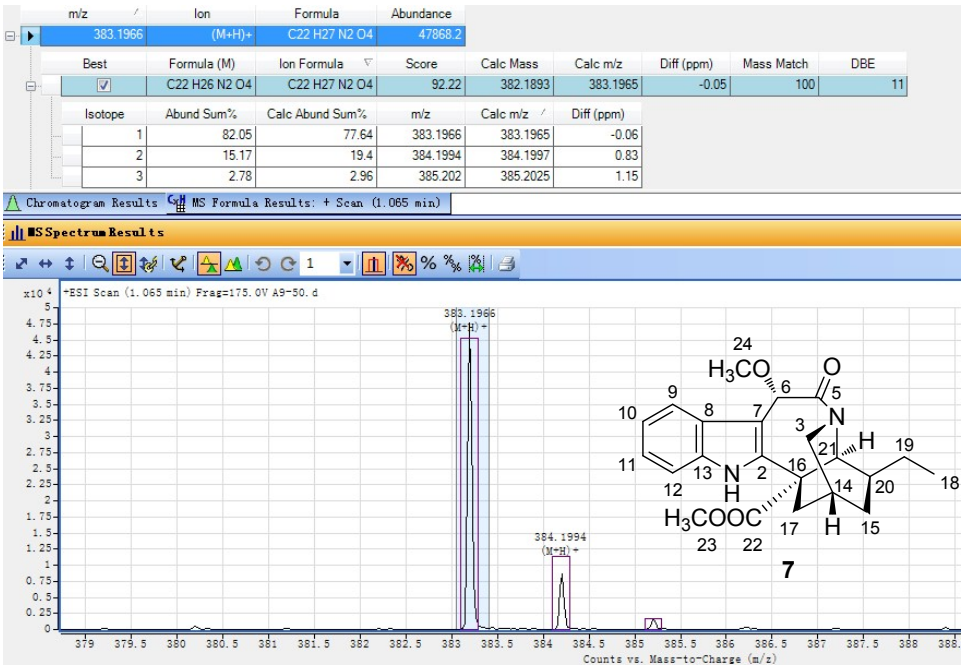

Fig. S77 HR-ESI-MS spectrum of **7**

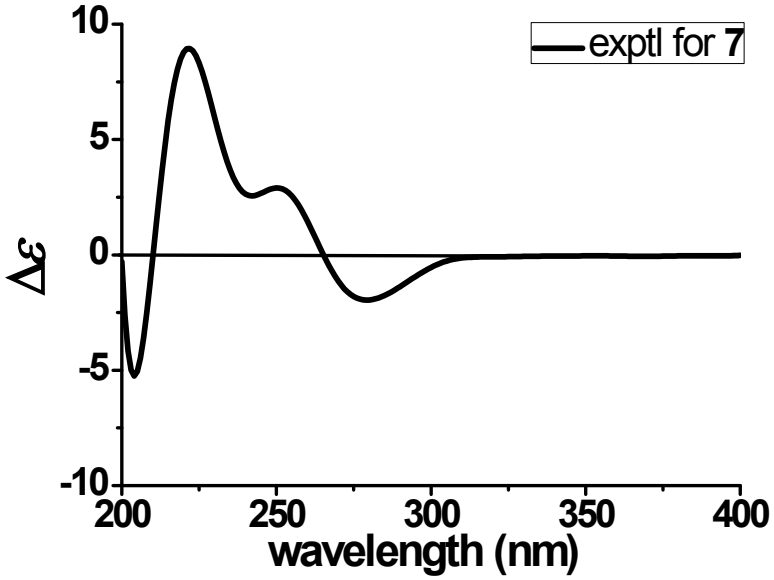

Fig. S78 CD spectrum of **7** (CH_3CN)

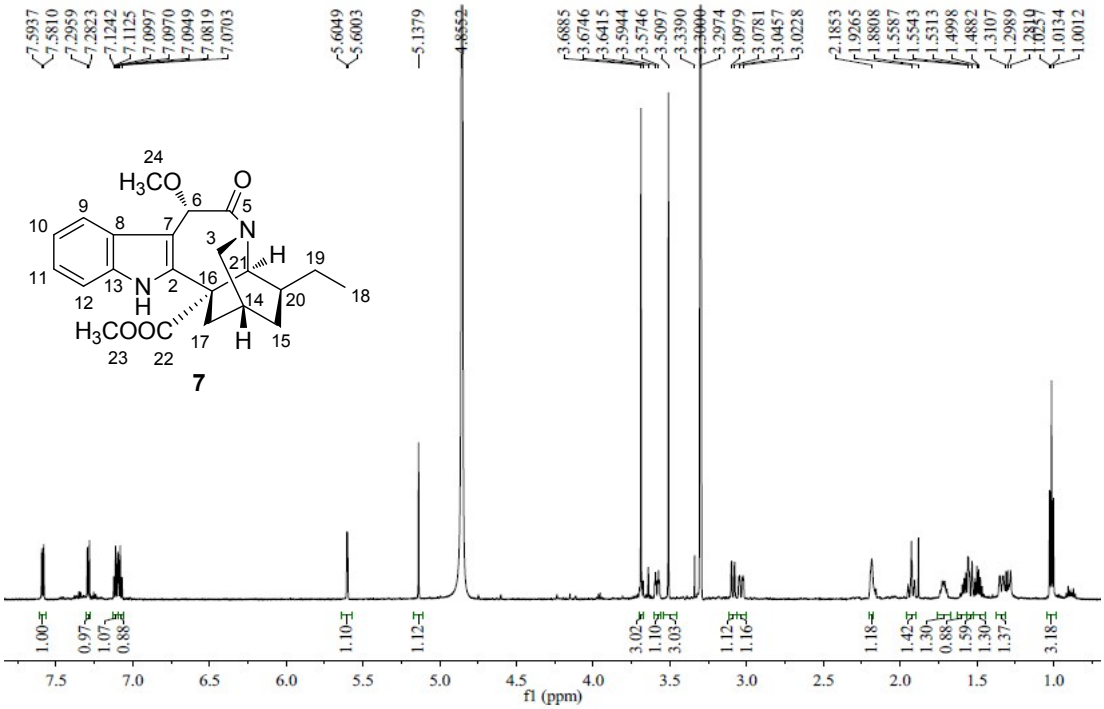

Fig. S79 ^{1}H-NMR spectrum of **7** (CD_3OD)

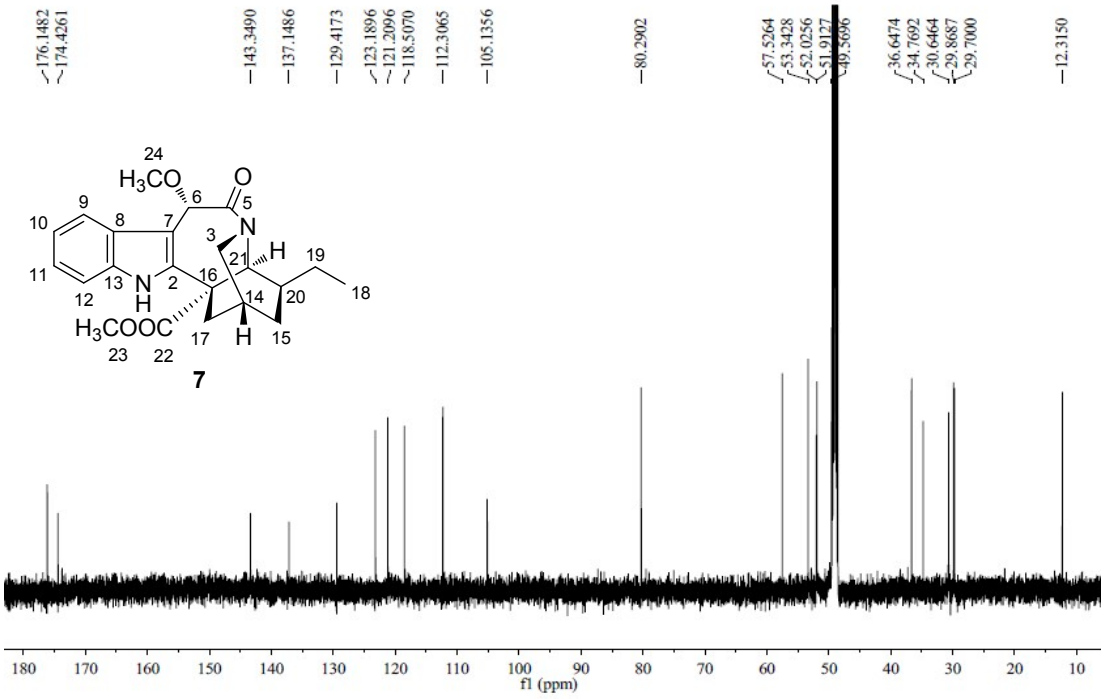

Fig. S80 ^{13}C-NMR spectrum of **7** (CD_3OD)

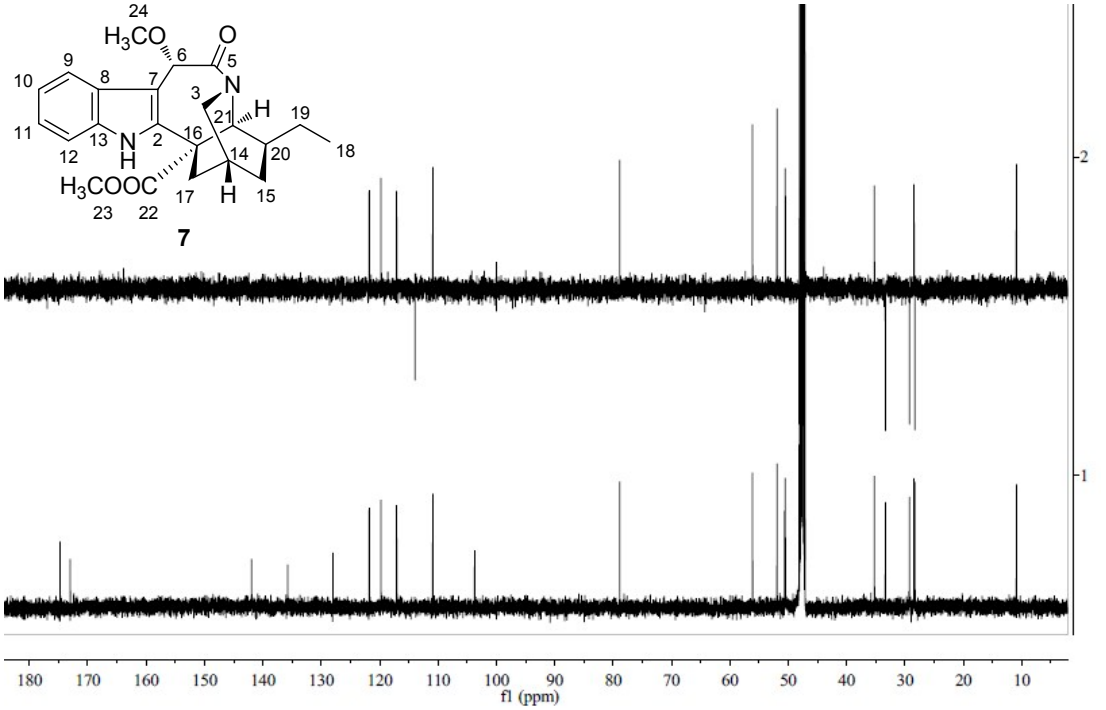

Fig. S81 DEPT-135 spectrum of **7** (CD_3OD)

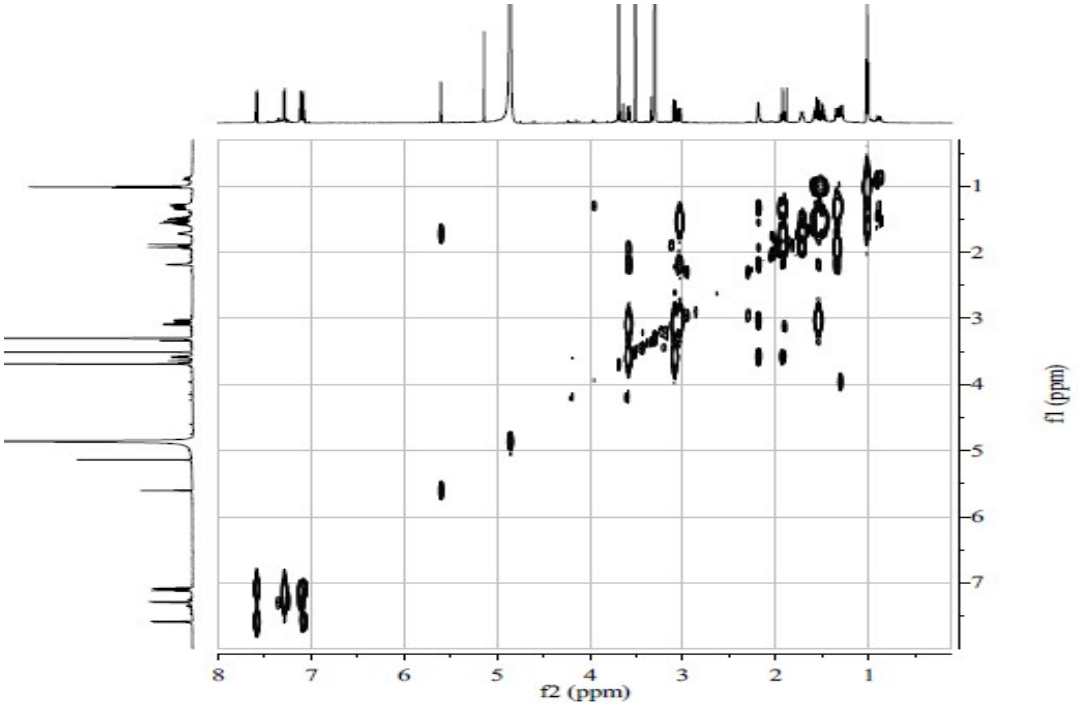

Fig. S82 ^{1}H-^{1}H COSY spectrum of **7** (CD_3OD)

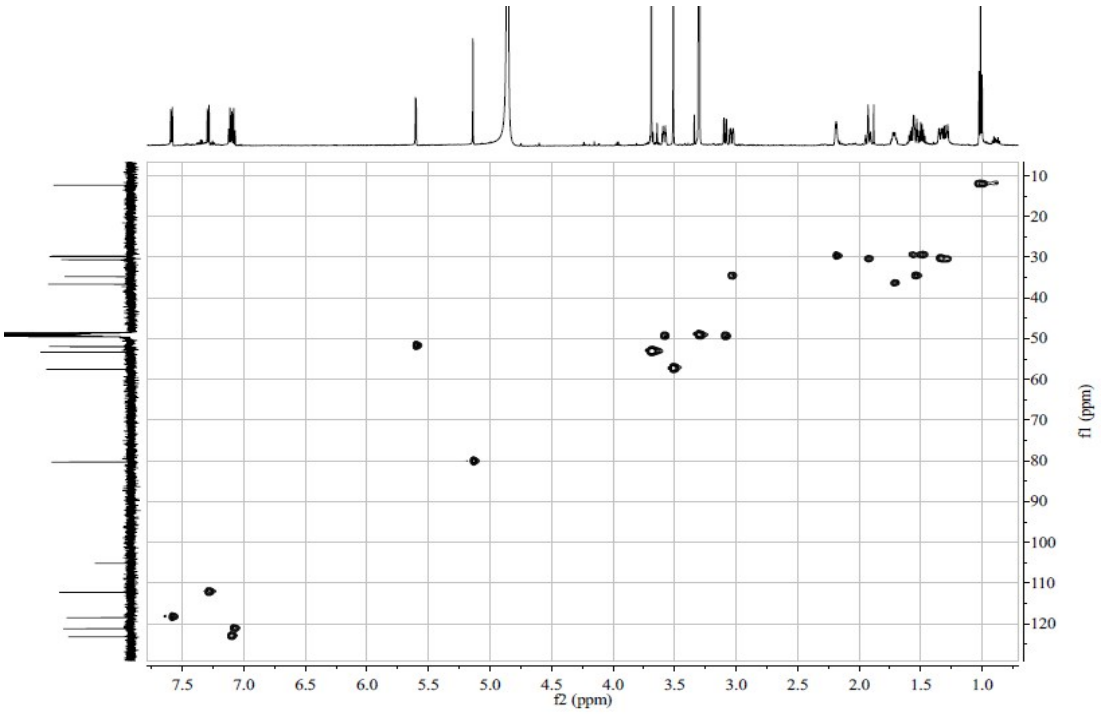

Fig. S83 HSQC spectrum of **7** (CD_3OD)

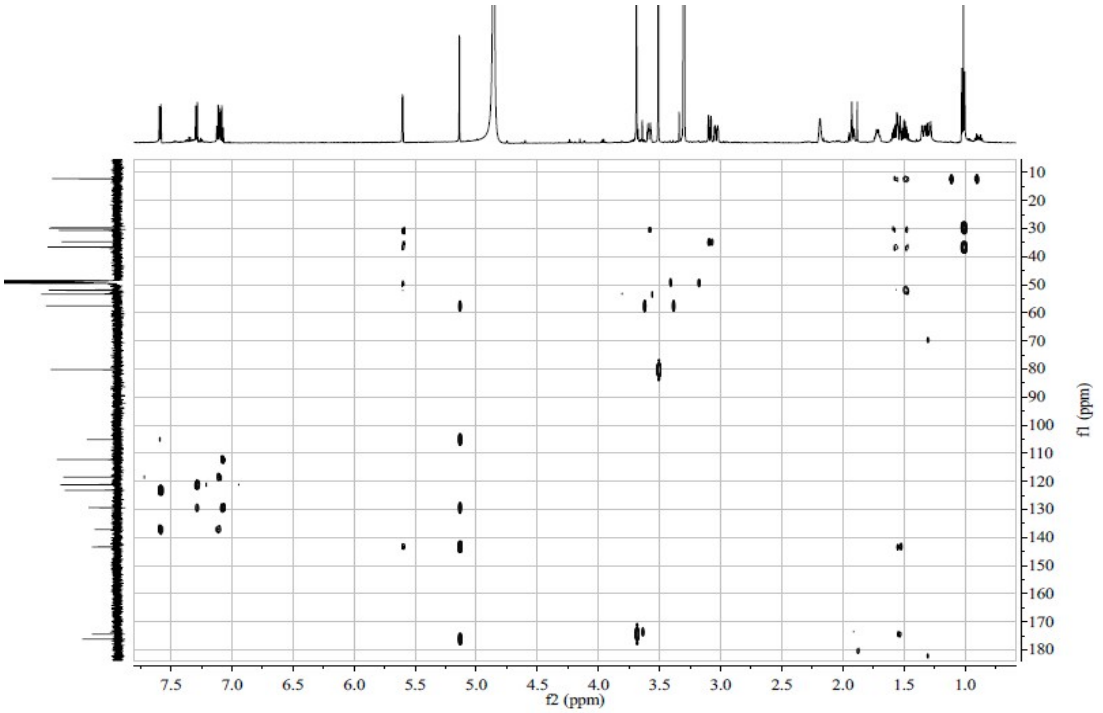

Fig. S84 HMBC spectrum of **7** (CD_3OD)

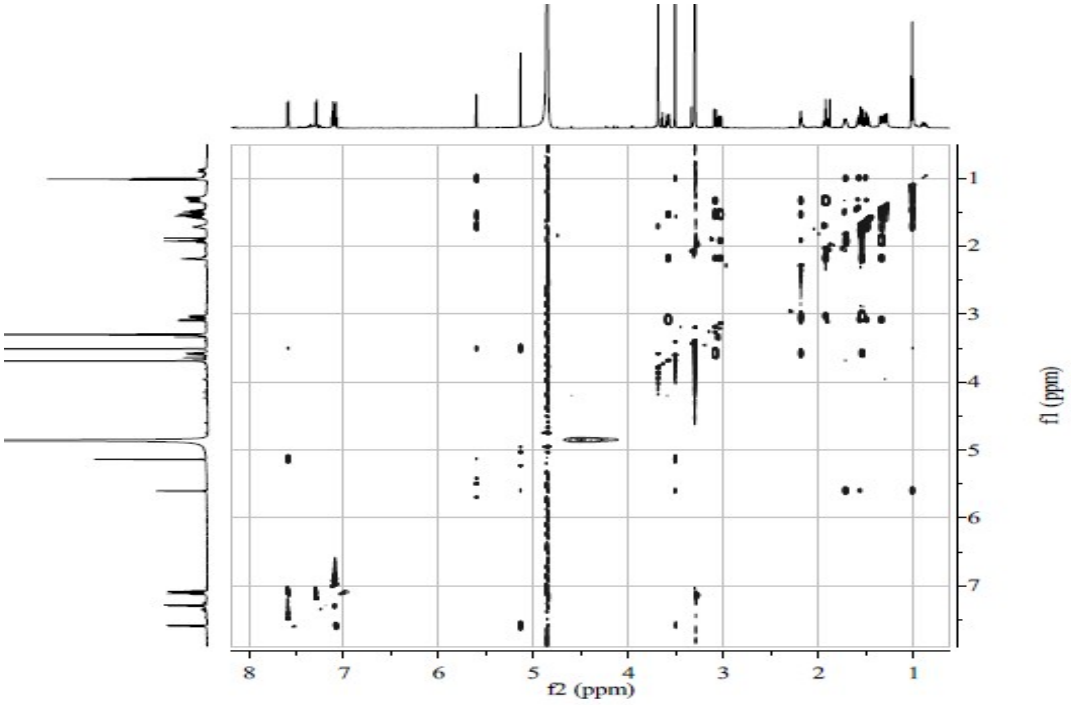

Fig. S85 NOESY spectrum of **7** (CD_3OD)